



Minerva Access is the Institutional Repository of The University of Melbourne

Author/s:

Saunders, GW;Filloramo, G;Dixon, K;Le Gall, L;Maggs, CA;Kraft, GT

Title:

Multigene analyses resolve early diverging lineages in the Rhodymeniophycidae (Florideophyceae, Rhodophyta)

Date:

2016-08-01

Citation:

Saunders, G. W., Filloramo, G., Dixon, K., Le Gall, L., Maggs, C. A. & Kraft, G. T. (2016). Multigene analyses resolve early diverging lineages in the Rhodymeniophycidae (Florideophyceae, Rhodophyta). *Journal of Phycology*, 52 (4), pp.505-522. <https://doi.org/10.1111/jpy.12426>.

Persistent Link:

<https://hdl.handle.net/11343/291452>

1

2 Received Date : 05-Jan-2016

3 Revised Date : 23-Mar-2016

4 Accepted Date : 09-Apr-2016

5 Article type : Regular Article

6

7

8 Multigene analyses resolve early diverging lineages in the Rhodymeniophycidae
9 (Florideophyceae, Rhodophyta)¹

10

11 *Gary W. Saunders*², *Gina Filloramo*, *Kyatt Dixon*

12 Centre for Environmental and Molecular Algal Research, Department of Biology,
13 University of New Brunswick, Fredericton, New Brunswick, E3B 5A3, Canada

14

15 *Line Le Gall*

16 Institut de Systématique, Évolution, Biodiversité, ISYEB – UMR 7205 – CNRS,
17 MNHN, UPMC, EPHE, Muséum national d’Histoire naturelle, Sorbonne Universités,
18 57 rue Cuvier, CP 39 75005, Paris, France

19

20 *Christine A. Maggs*

21 Faculty of Science and Technology, Bournemouth University, Poole House, Talbot
22 Campus, Poole, Dorset BH12 5BB, UK

23

24 *and Gerald T. Kraft*

This is the author manuscript accepted for publication and has undergone full peer review
but has not been through the copyediting, typesetting, pagination and proofreading
process, which may lead to differences between this version and the [Version of Record](#).

Please cite this article as [doi: 10.1111/IPY.12426-16-002](https://doi.org/10.1111/IPY.12426-16-002)

This article is protected by copyright. All rights reserved

25 School of Botany, University of Melbourne, Parkville, Victoria 1010, Australia

26

27 ¹Received ; accepted .

28 ²Author for correspondence: e-mail gws@unb.ca

29 Editorial Responsibility: H. Verbruggen (Associate Editor)

30 Running title: Rhodymeniophycidae phylogenyAbstract

31 Multigene phylogenetic analyses were directed at resolving the earliest divergences in
32 the red algal subclass Rhodymeniophycidae. The inclusion of key taxa (new to science
33 and/or previously lacking molecular data), additional sequence data (SSU, LSU, EF2,
34 *rbcL*, COI-5P), and phylogenetic analyses removing the most variable sites (site
35 stripping) have provided resolution for the first time at these deep nodes. The earliest
36 diverging lineage within the subclass was the enigmatic *Catenellopsis oligarthra* from
37 New Zealand (Catenellopsidaceae), which is here placed in the Catenellopsidales ord.
38 nov. In our analyses *Atractophora hypnoides* was not allied with the other included
39 Bonnemaisoniales, but resolved as sister to the Peyssonneliales, and is here assigned to
40 Atractophoraceae fam. nov. in the Atractophorales ord. nov. Inclusion of
41 *Acrothesaurum gemellifilum* gen. et sp. nov. from Tasmania has greatly improved our
42 understanding of the Acrosymphytales, to which we assign three families, the
43 Acrosymphytaceae, Acrothesauraceae fam. nov. and Schimmelmanniaceae fam. nov.

44

45 *Keyword index words:* Acrosymphytales, Acrothesauraceae, *Acrothesaurum*,
46 Atractophoraceae, Atractophorales, Catenellopsidales, Schimmelmanniaceae

47

48 *Abbreviations:* COI-5P, 5' region of the mitochondrial cytochrome oxidase subunit 1
49 gene; EF2, nuclear elongation factor 2 gene; LSU, nuclear large subunit ribosomal
50 DNA; *rbcL*, plastid ribulose-1,5-bisphosphate carboxylase/oxygenase large subunit
51 gene; SSU, nuclear small subunit ribosomal DNA

52

53

54 As with most lineages of living organisms, molecular data have come to play an
55 essential role in reshaping our understanding of organismal relationships and providing
56 new evolutionary perspectives for red algae (see Saunders and Hommersand 2004,

57 Yoon et al. 2006, Verbruggen et al. 2010). Among the five or six classes comprising
58 the phylum Rhodophyta (Saunders and Hommersand 2004, Yoon et al. 2006), the
59 Florideophyceae is by far the most species-rich, containing upwards of 95% of the
60 currently reported species (Guiry and Guiry 2015). The Florideophyceae consists of
61 multicellular marine and freshwater species currently assigned to five subclasses on the
62 basis of molecular and morphological analyses (Saunders and Hommersand 2004, Le
63 Gall and Saunders 2007). The subclass Rhodymeniophycidae contains some 75% of the
64 species currently assigned to the Florideophyceae (Guiry and Guiry 2015) including
65 many that are well known to non-specialists, e.g., Irish moss (*Chondrus crispus*
66 Stackhouse) and dulse [*Palmaria palmata* (Linnaeus) F. Weber & D. Mohr].

67 The Rhodymeniophycidae was established by Saunders and Hommersand
68 (2004) on the basis of molecular data available at that time (e.g. Saunders and Bailey
69 1997, 1999, Harper and Saunders 2001), as well as the key ultrastructural
70 synapomorphy of pit plugs that are covered by a cap membrane at their cytoplasmic
71 faces (Pueschel and Cole 1982). Saunders et al. (2004) completed a relatively
72 comprehensive molecular phylogenetic assessment of this subclass and established that
73 all orders except the Gigartinales were largely monophyletic, however, relationships
74 among most orders were unresolved. Saunders et al. (2004) included data for only the
75 SSU, for which varied rates of change in divergent lineages likely confounded
76 phylogenetic determinations (Le Gall and Saunders 2007). Subsequent research
77 included additional taxa and used the LSU and SSU in combination. As a result more
78 orders were recognized (e.g., Withall and Saunders 2006), but the relationships among
79 most of them remained equivocal. Indeed, of the 11 orders recognized in Withall and
80 Saunders (2006), only the positioning of the Halymeniales as sister to the Sebdeniales
81 and Rhodymeniales was consistently resolved. Studies using the *rbcL* have similarly
82 failed to resolve interordinal relationships (e.g., Gavio et al. 2005, Kravesky et al.
83 2009).

84 Attempts to resolve ordinal relationships among florideophycean subclasses then
85 took two divergent approaches. Le Gall and Saunders (2007) attempted to improve
86 resolution by adding taxa and generating sequence data for an additional nuclear
87 marker, EF2, whereas Verbruggen et al. (2010) used a data-mining approach to prepare
88 a supermatrix for phylogenetic analyses. Although support for monophyly of some

89 orders was improved and the subclass Corallinophycidae was recognized as distinct
90 from the Nemaliophycidae (Le Gall and Saunders 2007), relationships among orders of
91 the Rhodymeniophycidae remained poorly resolved. Verbruggen et al. (2010)
92 identified ordinal relationships among Rhodymeniophycidae as one of five poorly
93 supported regions in the red algal tree of life that were in need of further study. They
94 noted that “data availability for (this subclass) is meager to poor”, but provided
95 compelling evidence that resolution would be possible with the addition of more data
96 (Verbruggen et al. 2010, fig. 3). In the most recent effort, Yang et al. (2015) analyzed
97 mitochondrial genomes for 21 Rhodymeniophycidae. Again few novel interordinal
98 relationships were resolved with meaningful support except for an early divergence of
99 the Bonnemaisoniales, Gigartinales and Peyssonneliales relative to the remaining orders
100 (94% support in maximum likelihood analyses, Yang et al. 2015, fig. 1).

101 To improve the resolution of ordinal relationships within the
102 Rhodymeniophycidae we have generated data from more taxa, including some not
103 previously included in phylogenetic analyses, e.g., *Catenellopsis oligarthra* (J.Agardh)
104 V.J.Chapman, and more genes combining the five markers SSU, LSU, EF2, *rbcL*, and
105 COI-5P. We additionally completed analyses on alignments of progressively more
106 conservative characters (site stripping) in an effort to reduce the effects of saturation
107 and thus improve phylogenetic signal (Verbruggen 2012).

108

109 MATERIALS AND METHODS

110

111 *Molecular methods:* Samples for molecular investigation (Table S1 in the
112 Supporting Information) were processed and DNA extracted following Saunders and
113 McDevit (2012). Sequence data were generated for the SSU, LSU, EF2, *rbcL* and
114 COI-5P following Saunders and Moore (2013). Sequences were aligned using the
115 ClustalW plugin for Geneious R7 version 7.1.5 (<http://www.geneious.com>; Kearse *et al.*
116 2012) and included data from GenBank (Table S1). We generated five individual gene
117 alignments: SSU (68 taxa, 1702 of 1895 sites included in analyses; 93% complete);
118 LSU (72 taxa, 2605 of 3434 sites included in analyses; 99% complete); EF2 (67 taxa,
119 1681 sites; 92% complete); *rbcL* (69 taxa, 1358 sites; 95% complete) and COI-5P (65
120 taxa, 664 sites; 89% complete). In addition, a concatenated alignment for all taxa and

121 regions (73 taxa, 8010 aligned sites) was generated. Most taxa were at least 75%
122 complete except for *Acrosymphyton purpuriferum* (J.Agardh) G.Sjöstedt (54%
123 complete, data only for SSU and LSU) and *Pihiella liagoraciphila* Huisman,
124 A.R.Sherwood & I.A.Abbott (21% complete, data only for SSU), which together
125 accounted for ~26% of the missing data.

126 Single-gene alignments were analyzed with a GTR+I+G model, with
127 partitioning by codon for the three protein-coding genes, in the web-server program
128 RAxML (Stamatakis 2014) and robustness determined with 500 bootstrap replicates.
129 There were no strong inconsistencies noted among the single-gene trees and the five
130 genes were combined for phylogenetic analyses. Bayesian analysis was performed on
131 the full dataset using the MrBayes plugin for Geneious R7 version 7.1.5 under a
132 GTR+I+G model with parameter settings unlinked and the rates prior set to allow rate
133 differentiation across partitions (by gene and then by codon for protein-coding genes =
134 full partitioning scheme). This analysis was run twice for 1,000,000 generations with
135 sampling every 1000 generations. Plotting the overall likelihood against the number of
136 generations identified the stationary phase to determine the burn-in for each run.
137 Maximum likelihood analysis was performed under a GTR+I+G model with the data
138 fully partitioned using the RAxML plugin for Geneious R7 version 7.1.5 with 1000
139 bootstrap replicates.

140 Owing to the paucity of data for *Pihiella* (SSU only) the combined Bayesian
141 analyses were repeated after removing this taxon. There were no significant changes in
142 topology and only minor variations in posterior probability support indicating that its
143 inclusion was not negatively impacting our phylogenetic results.

144 To assess phylogenetic inference problems due to substitution saturation,
145 quickly evolving sites were calculated and systematically removed from the full
146 alignment. Site-specific rates were determined using the “substitution rates” analysis
147 tool in HyPhy (Pond et al. 2005) under the JC69 model with a Bayes phylogram as a
148 guide tree. To generate a series of progressively more conservative alignments the
149 program SiteStripper (Verbruggen 2012) was used to order the sites by rate then remove
150 the more rapidly evolving sites in increments of 5%. Maximum likelihood analysis
151 (ML) was performed on each “stripped” alignment (fully partitioned) using RAxML

152 version 7.3.5 with a command line script available through SiteStripper under a
153 GTR+I+G model and 1000 bootstrap replicates.

154 To assess how partitions might impact phylogenetic inference, the original
155 alignment and “stripped” alignments were analyzed by running PartitionFinder (Lanfear
156 et al. 2012) using the “greedy” algorithm under the BIC model selection method with
157 linked branch-length estimation. The best partitioning scheme and most appropriate
158 model of evolution as determined by PartitionFinder were subsequently used to
159 reanalyze the alignments with RAxML again with 1000 bootstrap replicates.

160

161 *Anatomical methods.* For anatomical observations, whole-mounts of gelatinous
162 species were made from liquid-preserved thallus fragments, and cross-sections of more
163 robust species were prepared from rehydrated or formalin-fixed samples by hand-
164 sectioning or in a cryostat (CM1850, Leica). Tissues were stained with 1% aniline blue
165 and mounted in 40-50% corn syrup. Observations were made with a light microscope
166 and documented with digital photography.

167 Morphological development of *Atractophora hypnoides* P.Crouan & H.Crouan
168 was followed in cultured material fixed in formalin-seawater (4%) and stained with
169 aniline blue acidified in 1% HCl. Cell nuclei were visualized by staining formalin-fixed
170 material in a drop of Hoechst 33258 solution ($10 \mu\text{g} \cdot \text{mL}^{-1}$) and examined with an
171 epifluorescence microscope (Leitz Dialux), or by staining with aceto-iron-
172 haematoxylin-chloral hydrate (Wittmann 1965) and photographed using Nomarski
173 interference, as described by Maggs (1989). Photographs were taken using Technical
174 Pan film developed in Kodak HC110 liquid developer.

175

176 *Culture studies.* *Atractophora hypnoides* was isolated from tetraspores released
177 by *Rhododiscus* tetrasporophytes collected at Finavarra, Co. Clare, Ireland, and Cloghy
178 Rocks, Strangford Lough, N. Ireland (multiple cultures were isolated from 1982-1986,
179 several of which were maintained long-term; see Maggs 1988). Cultures were grown in
180 half-strength modified von Stosch medium (Guiry and Cunningham 1984), at 15°C, in a
181 regime of 16:8 h light: dark (LD), under a photon irradiance of c. $20 \mu\text{mol photons} \cdot \text{m}^{-2}$
182 $\cdot \text{s}^{-1}$, and subject to changes in photoperiod as described in the text.

183

184 RESULTS

185

186 *Molecular phylogenetic analyses.* Topologies were congruent for all four analyses of
187 the full combined alignment (Bayes and maximum likelihood under full and
188 PartitionFinder partitioning) and the Bayesian result with partitioning by gene and
189 codon is presented (Fig. 1; with support values for all analyses summarized in Table 1).
190 Tree scores and branch support were typically slightly better for the fully partitioned
191 analyses, i.e., not using partitions identified by PartitionFinder (Table 1). To assess the
192 effects of substitution saturation a series of progressively more conservative alignments
193 were analyzed with maximum likelihood, again fully partitioned and with the schemes
194 determined by PartitionFinder. Consistent with the full combined alignment, tree scores
195 and overall support were typically better for analyses in which the data were fully
196 partitioned and only those values are presented (Table 1).

197 A neighbor-joining tree constructed with the HKY model was generated in
198 Geneious R7 (Fig. S1 in the Supporting Information) to determine if the starting tree
199 employed by HyPhy to determine individual site rates had biased downstream analyses.
200 These NJ-based site rates were used by SiteStripper to generate a series of
201 subalignments, which were analyzed in RAxML. The results of a Shimodaira-
202 Hasegawa test indicated that the neighbor-joining tree (likelihood -144264.31) was
203 significantly different ($p < 0.01$) from the Bayesian Inference tree (likelihood -
204 144682.75) used in the initial site-stripping analyses; however, use of the neighbor-
205 joining topology for calculating sites rates did not impact downstream site-stripping
206 analyses (data not shown).

207 In general terms support was moderate to strong at many key ordinal and
208 interordinal nodes, with some deeper nodes seeing enhanced support values at 10% site
209 removal (Table 1). Neither the Bonnemaisoniales nor Gigartinales was monophyletic
210 (Fig. 1; Table 1). *Catenellopsis oligarthra*, not previously included in phylogenetic
211 analyses, resolved as an independent lineage sister to the remainder of the
212 Rhodmeniophycidae and was not associated with other taxa assigned to the
213 Gigartinales (Fig. 1). The next diverging lineage was the fully supported
214 Bonnemaisoniales *sensu stricto* (Fig. 1), i.e., excluding *Atractophora hypnoides*, which
215 was resolved as sister to the strongly supported Peyssonneliales in a lineage with the

216 remaining Gigartinales (Fig. 1; Table 1). The remaining orders were resolved as a large
217 clade subdivided into two well-supported groups. The first of these consisted of
218 Acrosymphytales + Ceramiales + *Schmitzia* (Calosiphoniaceae). The novel Australian
219 taxon *Acrothesaurum gemellifilum* resolved within a fully supported lineage
220 encompassing species of the genera *Acrosymphyton* and *Schimmelmannia*, both
221 currently assigned to a single family in the Acrosymphytales (Fig. 1; Table 1). This
222 expanded Acrosymphytales was sister to the Ceramiales, which included with moderate
223 support the genus *Inkyuleea* (Fig. 1). Relationships among the Gelidiales, Gracilariales,
224 Nemastomatales, Plocamiales and the Halymeniales+Rhodymeniales+Sebdeniales
225 lineage remained largely unresolved, although some support for an alliance of the
226 Rhodymeniales+Sebdeniales was recognized (Fig. 1; Table 1). Finally, moderate
227 support was acquired for the continued inclusion of the Sarcodiaceae in the Plocamiales
228 (Fig. 1; Table 1).

229

230 *Taxonomic changes*

231

232 **Catenellopsidales** K.R.Dixon, Filloramo & G.W.Saunders, **ord. nov.**

233 *Description:* Thalli develop from triaxial apices. Gonimoblasts numerous,
234 arising from an extensive conjugated reticulum with associated nutritive tissue.

235 Tetrasporangia cruciate or decussate, terminal, embedded in outer cortical tissue.

236 *Type and only family:* Catenellopsidaceae Robins 1990, p. 698.

237

238 **Atractophorales** Maggs, L.Le Gall, Filloramo & G.W.Saunders, **ord. nov.**

239 *Description:* Gametangial thallus consisting of erect axes arising from a basal
240 disc; lubricous with erect branches spirally arranged; uniaxial with four periaxial cells
241 per whorl. Monoecious; carpogonial branches 3-celled; procarpic, supporting cell
242 functioning as auxiliary cell, fusing with the fertilized carpogonium, from which the
243 gonimoblast arises. Gonimoblast a diffuse system of loose descending filaments,
244 forming a covering around one or more cells of the main axis; pericarp absent. Mature
245 cystocarps spindle-shaped. Spermatangia in superficial clusters. Tetrasporangial
246 thallus crustose; tetrasporangia regularly cruciate, terminal.

247 *Type and only family:* Atractophoraceae Maggs, L.Le Gall & G.W.Saunders,
248 fam. nov.

249

250 **Atractophoraceae** Maggs, L.Le Gall & G.W.Saunders, **fam. nov.**

251 *Description:* as for Atractophorales.

252 *Type genus:* *Atractophora* P.Crouan & H.Crouan 1848: 371.

253 ■ *Additional genus:* *Liagorothamnion* Huisman, D.L.Ballantine & M.J.Wynne,
254 2000: 507, 508 (discussed below).

255 *Lectotypification:* *Atractophora hypnoides* was provisionally lectotypified by
256 Dixon and Irvine (1977) in CO. The collection of the brothers Crouan contains five
257 specimens of *Atractophora hypnoides*, as well as an illustration (IC BOT/Herb.
258 CO/0001) with a fragment of a plant (CO00287). None of the specimens accord with
259 the protologue, which mentioned a specimen dredged at 8-10 m depth on August 20th
260 1848 in the Rade de Brest and growing on *Melobesia polymorpha* (Linnaeus) Harvey
261 and on *Ceramium rubrum* C.Agardh. Among the five specimens, one lacks collection
262 information (CO00289), one is from Noirmoutier (CO00291), and the remainder are
263 from the Rade de Brest. Among the last, one has no collection date (CO00290) and the
264 other two were collected at Baie Sainte Anne in 1847. Specimen CO00288 was
265 growing on *Ceramium*, a host mentioned in the protologue. We therefore designate
266 specimen CO00288 as the lectotype of *Atractophora hypnoides* (Fig. 2).

267 *Gametophyte observations in culture:* *Atractophora hypnoides* tetraspores form
268 small multicellular loosely coherent discs that give rise centrally to an erect axis. Erect
269 axes consist initially of a single filament produced by transverse divisions of a more or
270 less isodiametric apical cell. Beginning at about the sixth cell from the apex, each axial
271 cell cuts off a periaxial cell from a lateral protuberance. Alternate axial cells give rise to
272 two periaxial cells/whorl branch initials at 180° to each other, initially forming a
273 distichous arrangement of branchlets (Fig. 3a). As axes develop further, periaxial cells
274 are also cut off at 90° to the first branchlets, resulting in whorls of four branchlets of
275 limited growth in a cruciate arrangement (Fig. 3b). Axial cells enlarge greatly in length
276 and diameter, mainly below the insertion of the whorl, so that the whorl is eventually
277 positioned around the distal part of the axial cell, all enclosed in a thin (<10 µm)
278 mucilaginous sheath (Fig. 3, b and d). Whorl branchlets consist of inflated cells 10 µm

279 in diameter, tapering to cylindrical/conical apical cells that often bear hairs up to 100
280 μm long (Fig. 3c). Occasional whorl branchlets are replaced by axes of indeterminate
281 growth, of the same construction as the primary axis, but generally forming the cruciate
282 arrangement of whorl branchlets within the apical 10-12 axial cells (Fig. 4a).

283 When about one month old, thalli start to produce a distichous arrangement of
284 lateral ramuli from the whorl branchlets, and axes develop a filamentous cortication
285 formed by down-growing rhizoidal filaments that originate from the basal cell of every
286 whorl branchlet (Fig. 3d). All vegetative cell types are uninucleate and contain irregular
287 ribbon-like to reticulate chloroplasts; neither secondary pit connections nor cell fusions
288 are formed.

289 At about 1.5 months old, thalli form spermatangia and carpogonial branches just
290 below the apices of axes (Figs. 3, e-j and 4, a-e). Spermatangia develop in dense
291 clusters all around axes, arising from modified whorl branchlets, each cell of which cuts
292 off small spermatangial mother cells in all directions, singly or in chains.

293 Spermatangial mother cells are rectangular/pyriform and by oblique divisions cut off 2-
294 3 uninucleate spermatangia 1.5-2 μm long (Figs 3e, 4b). Released spermatia are
295 spherical, uninucleate and 2.5-3 μm in diameter (Fig. 4c).

296 Carpogonial branches usually develop from the basal cell of a modified whorl
297 branch, which is thus the supporting cell (Figs 3f-j, 4d-e). The carpogonial branch is 3-
298 celled, the carpogonium and hypogynous cell lying at right angles to the first branch
299 cell, which brings the carpogonium close to the supporting cell (Fig. 4, d and e). The
300 supporting cell bears a 1-celled and a 2-celled lateral branch, and the first cell of the
301 carpogonial branch also bears a lateral cell, forming together an 8-celled structure (Figs.
302 3j and 4e). The carpogonium is triangular as one side lies along the hypogynous cell,
303 and another along the first carpogonial branch cell. The trichogyne develops from the
304 third side, towards the axis at first, and then bending outwards and growing to about 250
305 μm in length (Figs. 3, f-i and 4, d and e). The cytoplasm of the trichogyne is constricted
306 near the carpogonium and then expands to about 2 μm wide, surrounded by a mucilage
307 sheath 2 μm thick. Numerous spermatia are observed on hairs and trichogynes, forming
308 cytoplasmic continuity with the trichogynes (Figs. 3k and 4c).

309 Following fertilization, the carpogonium and supporting cell fuse to form a
310 dumb-bell shaped cell in some cases, with the hypogynous cell remaining separate (Fig.

311 4h). In other examples the carpogonium and hypogynous cell appear to fuse before
312 joining with the supporting cell. It appears that the first carpogonial branch cell
313 sometimes becomes part of the fusion cell (Fig. 4, f and g). An additional fusion can
314 occur between two of the lateral cells, but this fusion cell is separate from the one
315 involving the carpogonium (Fig. 4, f and g). Early post-fertilization development is
316 apparently quite variable but is obscured by the production of dense clusters of small
317 “nutritive” cells by the first carpogonial branch cell, its lateral cell, and the hypogynous
318 cell (Figs. 3j and 4, f-h). These persist as a small group of cells attached to the fusion
319 cell(s). The fusion cell formed from the carpogonium and the supporting cell cuts off a
320 gonimoblast initial from the carpogonium end (Figs. 3l and 4, f and g). The
321 gonimoblast initial quickly gives rise to several non-pigmented branched gonimoblast
322 filaments, which surround the axis, weaving amongst the whorl branchlets and giving
323 rise to radiating filaments (Fig. 4i). Deeply pigmented carposporangia 12-13 μm in
324 diameter are borne terminally on these outward-growing filaments (Figs. 3m and 4i).
325 Approximately 1.5 months after the first appearance of gametangia, globular mature
326 cystocarps about 250 μm in diameter are present, often arranged in series on an axis due
327 to its continued growth and formation of carpogonial branches.

328 *Tetrasporophyte observations:* Carpospores of about 20 μm diameter released in
329 culture and grown under the same conditions as field-collected tetraspores (i.e., 15°C;
330 16:8h LD) germinate in the same manner as the tetraspores to produce cohesive discs
331 (Fig. 5a). Basal layer filaments of crusts branch pseudodichotomously (Fig. 5c),
332 forming a polyflabellate pattern due to the cessation of growth of most filaments soon
333 after branching, causing considerable variation in cell dimensions. This pattern is also
334 seen in field material of *Rhododiscus pulcherrimus* P.Crouan & H.Crouan (Fig. 5f), and
335 results in a lobed or irregular margin. No cell fusions or secondary pit connections are
336 formed; calcification is absent. Three months after germination, crusts are up to 2 mm
337 in diameter and 30 μm thick, including a thick mucilage layer on the upper and lower
338 surfaces. They consist of basal layer cells, each bearing one or two 5-6 celled erect
339 filaments 8-14 μm in diameter (Fig. 5d). The cell cut off behind the apical cell of a
340 basal layer filament immediately divides periclinally (Fig. 5b) to form crust margins
341 two cells thick. No erect axes developed from these crusts. Crusts transferred to 15°C;
342 8:16h LD and then to 10°C; 8:16h LD formed tetrasporangia across the surface,

343 developing from the darkly pigmented apical cells of the erect filaments (Figs 5d, e).
344 Tetrasporangia are regularly cruciately divided (Fig. 5d), c. 16-20 μm in length and
345 diameter, smaller and rounder than in field-collected material (Fig. 5f), in which they
346 are 16-37 x 10-20 μm . In culture, tetrasporangia release tetraspores about a month after
347 formation.

348

349 Acrosymphytales Withall & G.W.Saunders 2006, p. 389-390.

350 *Type family:* Acrosymphytaceae S.C.Lindstrom 1987, p. 52.

351 *Type genus:* *Acrosymphyton* G.Sjöstedt 1926, 8-9.

352

353 **Acrothesauraceae** G.W.Saunders & Kraft, **fam. nov.**

354 *Description:* Thalli uniaxial, apical cell division transverse, the central-axial
355 cells each bearing nodal whorls of sub-/pseudodichotomous determinate laterals.
356 Carpogonial and auxiliary-cell filaments both simple, occurring singly, in pairs or in
357 clusters. Diploidization of the auxiliary cells effected by direct fusion with a
358 presumably fertilized carpogonium, or its derivative cell, in the same (procarpic) or a
359 separate (nonprocarpic) branch system. Tetrasporophytes unknown.

360 *Type genus:* *Acrothesaurum* Kraft & G.W.Saunders, gen. nov.

361 *Additional genus:* *Peleophycus* I.A.Abbott 1984, 325-327 (discussed below).

362

363 ***Acrothesaurum*** Kraft & G.W.Saunders, **gen. nov.**

364 *Description:* Thalli flaccid, lubricous; central-axial cells each bearing nodal
365 whorls of sub-/pseudo-dichotomous determinate laterals; mid and lower axes corticated
366 between nodal whorls by branched, basipetally directed rhizoids. Thalli monoecious;
367 spermatangia borne directly on terminal and subterminal cells of whorl branchlets;
368 carpogonial and auxiliary-cell filaments both unbranched, occurring singly, in pairs or
369 in clusters on periaxial and one or two distal cells of whorl branchlets, directed
370 basipetally, the auxiliary cells terminal. Diploidization of auxiliary cells effected by
371 direct fusion with presumably fertilized carpogonia, the diploidized auxiliary cell either
372 borne on the same supporting cell as the donor carpogonium (procarpic) or on one of
373 several adjacent supporting cells (nonprocarpic); gonimoblast initials single,
374 carposporophytes composed of up to three synchronously maturing gonimolobes

375 consisting entirely of carposporangia. Proximal portions of diploidized auxiliary cells
376 frequently emitting one or two stout, basally directed filaments that fuse apically to
377 central-axial cells and/or adjacent lower whorl-branchlet cells. Tetrasporophytes
378 unknown.

379 *Etymology*: from “acro”, referring to objects at an extremity, and “thesaurum”,
380 for a treasury or treasure chamber, in reference to the terminal auxiliary cells that
381 receive and house the “precious” zygote nucleus that initiates the embryonic
382 carposporophyte.

383 *Type and only species*: *Acrothesaurum gemellifilum* Kraft & G.W.Saunders, sp.
384 nov.

385
386 ***Acrothesaurum gemellifilum* Kraft & G.W.Saunders, sp. nov.** Figures 6-8

387 *Description*: portion of thallus on holotype slide (Fig. 6a) banded, 14 mm in
388 height, 17.8 mm in width, the whole specimen (Fig. 6b) lubricous, 60 mm in height, 73
389 mm in greatest breadth, erect from a holdfast pad of consolidated rhizoidal filaments;
390 axes terete (Fig. 6, c and j), irregularly radially branched to four orders, indeterminate
391 lateral initials scattered (Fig. 6c), arising on epi-periaxial cells of determinate whorl-
392 laterals (Fig. 6d); proximal axes to 1600 μm in diameter, 550-650 μm in lower first-
393 order laterals, narrowing to 10-20 μm at gradually tapered tips (Fig. 6c). Cells of
394 central-axial filaments 60-90 μm long, 18-25 μm wide (Fig. 6d), each with (3-)4
395 periaxial cells at distal poles, the periaxial cells subtending a determinate
396 subdichotomous whorl branchlet with domed or lacrimiform (Fig. 6, c and d),
397 sometimes hair-terminated (Fig. 6e), apical cells, the nodal appearance of fronds
398 accentuated by the regular spacing of adjacent whorls (Fig. 6, a and d). Rhizoidal
399 filaments basipetal, 2-4 μm in diameter, initially simple (Fig. 6f), later branched (Fig.
400 6g), mostly arising from periaxial cells, also frequently from apical and subapical cells
401 of apparently non-functioning carpogonial and auxiliary-cell branches, in mature axes
402 issuing adventitious filaments perpendicularly to fully corticate the central-axial cells
403 between adjacent whorl-branch nodes (Fig. 6h). Spermatangia spherical, 2.0-2.5 μm in
404 diameter, borne singly or usually in pairs or threes (occasionally fours) mostly on
405 terminal cells of whorl-branchlets (Fig. 6, i and j), less frequently also singly or in pairs
406 on subterminal cells. Carpogonial and auxiliary-cell branches basipetally directed

407 (Figs. 6, f and I and 7, a-c), borne individually and intermixed on periaxial or epi-
408 periaxial supporting cells (Fig. 7b), the auxiliary-cell branches usually three-celled,
409 predominant (Fig. 7, a and b), the carpogonial branches scarcer, normally four-celled
410 (Fig. 7, a-c), rarely five-celled (Fig. 7d), the carpogonia campanulate and with straight
411 (Fig. 7, c and d) or sinuous (Fig. 7e) trichogynes, the carpogonia usually borne on an
412 inflated, subspherical to ovoid hypogynous cell c. 7.5-8 μm x 6 μm (Fig. 7, b-e);
413 carpogonia frequently non-functional, at various stages of breaking down (Fig. 7, b and
414 e), carpogonial branches then resembling three-celled auxiliary-cell branches because
415 hypogynous cells are the size and shape of auxiliary cells (Fig. 7, b and e). Auxiliary
416 cells terminal, usually ovoid (Fig. 7a-c), 6-15 x 6-9 μm in diameter; each functional
417 carpogonial branch invariably associated with an adjacent auxiliary-cell branch on the
418 same or an adjoining supporting cell (Fig. 7, a-c). Diploidization of auxiliary cells
419 effected by direct fusion of the presumably fertilized carpogonium (Fig. 7, f and g), the
420 auxiliary cell enlarging, becoming eccentrically swollen (Fig. 8, a and b) and cutting off
421 a single terminal gonimoblast initial (Figs. 7g and 8a). Gonimolobes compact, the
422 auxiliary cell elongating, thickening distally (Fig. 8, b-d), darkly staining (Fig. 8, a-e),
423 frequently initiating two stout single-celled arms of undetermined function proximal to
424 the carposporophyte (Figs. 7h and 8, d and e), the arms ultimately fusing apically with
425 central-axial cells (Fig. 8, b and d). Carposporophytes globular (Figs. 7h and 8, c and
426 e), at maturity 250-450 μm in diameter and composed of three compact synchronously
427 maturing gonimolobes of carposporangia (Fig. 8f), the gonimolobes consisting of
428 tightly folded filaments of pit-connected subspherical to angular carposporangia 25-50
429 μm in diameter.

430 *Etymology*: from “gemellus” (paired or twinned), and “filum” (filament), in
431 reference to the adjacency of carpogonial and auxiliary-cell filaments that connect after
432 fertilization either procarpically or nonprocarpically.

433 *Holotype*: GWS016355, slide A (Fig. 6a). The holotype slide and six duplicate
434 slides (GWS016355B-G) permanently housed at UNB. Habit of the entire type
435 specimen was photographed before it was dried in silica as a voucher (Fig. 6b).

436 *Type locality*: Wynyard, Tasmania (40° 58' 48.7" S; 145° 45' 04" E), -12 m on
437 shell at Sanctuary Reef (G.W. Saunders & K.R. Dixon, 28 Jan. 2010).

438 *Distribution*: known only from the single holotype specimen.

439

440 **Schimmelmanniaceae** G.W.Saunders & Kraft, **fam. nov.**

441 *Description:* Thalli uniaxial, apical cell division transverse, the central-axial
442 cells each bearing nodal whorls of sub-/pseudodichotomous determinate laterals.
443 Procarpic; carpogonial and auxiliary-cell branches in pairs on supporting cells.
444 Diploidization of auxiliary cells effected by direct fusion with presumably fertilized
445 carpogonia, typically following division of the latter. Tetrasporophytes crustose;
446 tetrasporangial division cruciate.

447 *Type genus:* *Schimmelmannia* Schousboe ex Kützing, 1849: 722.

448 *Additional genus:* *Gloeophycus* I.K.Lee & S.A.Yoo 1979, p. 347 (discussed
449 below).

450

451 DISCUSSION

452

453 The combination of more taxa, notably some key lineages previously poorly
454 studied or newly discovered, additional sequence data and exploration of phylogenetic
455 analyses that account for site saturation have resulted in increased resolution among the
456 deep-diverging lineages of Rhodmeniophycidae. This problematic portion of the red
457 algal tree of life (Withall and Saunders 2006) was considered solvable in the analyses of
458 Verbruggen et al. (2010), which was consistent with the results here. Phylogenetic
459 reconstruction can be difficult when sequences become saturated and when deep
460 evolutionary events have occurred in relatively close succession such that the available
461 signal is masked by noise in an alignment. Site stripping as performed here can
462 enhance the signal to noise ratio improving phylogenetic inference (Verbruggen 2012).
463 Logically, a node of interest in evolutionary time will be impacted such that resolution
464 of deeper nodes could see greater improvement with more site removal relative to more
465 recent nodes. However, as more and more sites are removed signal will also be
466 removed and support across the phylogeny will degrade. Although stochastic events can
467 complicate matters, the previous patterns were generally observed in our analyses (Fig.
468 1; Table 1). As with many studies Bayesian posterior probabilities were typically
469 higher in support of various relationships than were the corresponding ML bootstrap
470 percentages (Table 1). Although the former values are typically considered to

471 overestimate support (see Wróbel 2008), our analyses of progressively more
472 conservative alignments showed enhanced ML bootstrap support for relationships with
473 high posterior probability support in our original analyses of the full alignment (Table
474 1). For the current alignment and model at least, higher posterior probabilities in
475 analyses of the full alignment appeared to be indicative of phylogenetic signal for the
476 resolved relationships (e.g., Table 1 nodes E and H), i.e., Bayesian posterior
477 probabilities may have been more indicative of evolutionary relationships when the full
478 alignment was analyzed than were the ML bootstrap values. It should also be noted that
479 the latter values are typically considered as conservative estimators of support (Wróbel
480 2008). Although the general applicability of site stripping for enhancing phylogenetic
481 resolution awaits more study, the novel phylogenetic insights generated here have
482 necessitated a suite of taxonomic changes at the familial and ordinal levels to represent
483 the full diversity of the lineages under study and to adhere to the principle of
484 monophyly.

485 Agardh (1876) originally described *Catenellopsis oligarthra* as a species of
486 *Catenella*, at the time placed in the Solieriaceae. Kylin (1932) transferred it to
487 *Nemastoma* based on tetrasporangial anatomy, but Chapman (1979) later described the
488 new genus *Catenellopsis* (Gymnophloeaceae/‘Nemastomataceae’) because the
489 carposporangia were formed strictly in constricted regions of the saccate thalli. Later,
490 when erecting the monospecific family Catenellopsidaceae, Robins (1990) compared
491 the reproductive anatomy of *C. oligarthra* to several other families. Although he did
492 not observe carpogonia or early post-fertilization development, Robins (1990)
493 considered the post-fertilization anatomy of *C. oligarthra* to be so distinct that even its
494 ordinal position was uncertain. Nevertheless Robins (1990) provisionally retained
495 *Catenellopsis* and the Catenellopsidaceae in the Gigartinales. Our molecular data, the
496 first published for this species, resolved *Catenellopsis* as an isolated lineage sister to the
497 remainder of the Rhodymeniophycidae necessitating the recognition of this taxon at the
498 ordinal level.

499 Members of the Bonnemaisoniaceae (represented by *Asparagopsis* and *Delisea*)
500 and two members of the Naccariaceae (*Naccaria* and *Reticulocaulis*) group together
501 (although the Bonnemaisoniaceae is paraphyletic and further familial level study is
502 needed in this order), but *Atractophora*, previously assigned to the Naccariaceae, does

503 not join this clade (Fig. 1). The systematic position of *Atractophora* has long been
504 debated. In describing *A. hypnoides* Crouan and Crouan (1848) posited an alliance with
505 *Dudresnaya*. Agardh (1863) transferred this species to *Naccaria*, which he placed in his
506 family Wrangelieae (although given the rank of 'ordo' Agardh's name was equivalent to
507 a family), while Zerlang (1889) again recognized *Atractophora* as a distinct genus.
508 Schmitz and Hauptfleisch (1897) allied *Atractophora*, *Naccaria* and *Wrangelia* in the
509 Wrangelieae of the family Gelidiaceae, with Oltmanns (1904) soon after recognizing
510 the family Wrangeliaceae for these three genera. Kylin (1928) erected the Naccariaceae
511 to include *Naccaria* and *Atractophora*. He discussed the relationships of the
512 Naccariaceae and suggested, based on post-fertilization development, that the family
513 was allied to the Bonnemaisioniaceae, which at that time was included in the Nemaliales
514 (as Nemalionales). Feldmann and Feldmann (1942) separated the Bonnemaisioniaceae
515 from the Nemaliales owing to the heteromorphic life cycle of *Asparagopsis* and
516 *Bonnemaisionia* and proposed the Bonnemaisioniales. Kylin (1956) did not recognize
517 the Bonnemaisioniales and included the Naccariaceae (including *Atractophora*,
518 *Naccaria* and *Neoardissonia*) and Bonnemaisioniaceae (including *Asparagopsis*,
519 *Bonnemaisionia*, *Delisea*, *Leptophyllis* and *Ptilonia*) at the end of his treatment of the
520 Nemaliales (as Nemalionales).

521 Fan (1961), discussing relationships of the Gelidiales, stressed a major
522 difference between *Atractophora* and *Naccaria* in that the nutritive filaments associated
523 with carpogonial branches were produced by the supporting cell versus the hypogynous
524 cell, respectively. Fan considered that both genera displayed direct development of the
525 gonimoblast from the carpogonium like the Gelidiales, and felt that the
526 Bonnemaisioniaceae should be recognized at the ordinal level, as proposed by Feldmann
527 and Feldmann (1942). However, Papenfuss (1966) and Dixon and Irvine (1977)
528 continued to place the Bonnemaisioniaceae in the Nemalionales.

529 Pueschel and Cole (1982) showed that both *Atractophora hypnoides* and
530 *Bonnemaisionia hamifera* Hariot have pit plugs characterized by a membrane only and
531 lacking plug caps, whereas *bona fide* Nemaliales have two-layered plug caps. They
532 considered this as strong evidence in support of the Bonnemaisioniales as distinct from
533 the Nemaliales and continued to include the Bonnemaisioniaceae and Naccariaceae in
534 the former order. However, it is important to note that this pit-plug type is shared by

535 virtually all Rhodymeniophycidae and provides no evidence on the relationships
536 between these two families and the many orders of this subclass (Saunders and
537 Hommersand 2004). Womersley (1996) speculated that the Naccariaceae may not be
538 related to the Bonnemaisoniaceae owing to significant differences in the reproductive
539 structures including the diffuse rather than compact gonimoblast and the complete
540 absence of a pericarp.

541 ■ Separation of *Atractophora* from the rest of the Naccariaceae is not entirely
542 unexpected despite similarities of the uniaxial mucilaginous erect gametophytes and
543 mature carposporophytes composed of diploid tissue tightly surrounding the primary
544 axis, intermixed with sterile filaments, and lacking a consolidated pericarp. There are
545 several potentially significant vegetative differences, such as the transverse apical cell
546 division in *Atractophora* (Fig. 3c) compared to the oblique division in *Naccaria* (Kylin
547 1928, fig. 7A) and *Reticulocaulis* (Schils et al. 2003, fig. 23), the number of periaxial
548 cells cut off each axial cell (four in *Atractophora* versus two in members of the
549 Bonnemaisoniales *sensu stricto*), and the absence of secondary pit connections in
550 *Atractophora* (Figs. 3d and 5c) versus their presence in *Naccaria* and *Reticulocaulis*
551 (Schils et al. 2003). There are many similarities in female development between
552 *Atractophora* and *Naccaria*, such as the presence of nutritive-cell clusters on the
553 carpogonial branch (Kylin 1928, Chihara and Yoshizaki 1972, Hommersand and
554 Fredericq 1990), which was the basis of their association with the Bonnemaisoniaceae.
555 However, there are also significant differences between the early post-fertilization
556 development of *Atractophora* and the other Naccariaceae, the most important of which
557 is that whereas in *Atractophora* the supporting cell (= auxiliary cell) fuses with the
558 fertilized carpogonium (Fig. 4h), in *Naccaria* and *Reticulocaulis* it remains discrete
559 (Kylin 1928, Schils et al. 2003). As reported by Kylin (1928), in *Atractophora* the
560 gonimoblast develops from the carpogonial element of the fusion cell (Fig. 4g), not
561 from the auxiliary cell. We have also observed fusion between the carpogonium and
562 hypogynous cell (Fig. 4g), and among some of the lateral (nutritive) cells, which was
563 not reported by Kylin (1928), but resembles that in *Reticulocaulis* in which the fertilized
564 carpogonium fuses directly with the hypogynous cell via the expansion or breakdown of
565 the pit connection (Schils et al. 2003).

566 *Atractophora hypnoides* resolved distant from the included Bonnemaisoniales
567 and as sister to the Peyssonneliales (Fig. 1). The sister relationship observed between
568 *Atractophora* and the Peyssonneliales was unexpected and intriguing, particularly
569 considering their contrasting morphologies and the anatomical similarities that
570 *Atractophora* shares with members of the Naccariaceae (Bonnemaisoniales), to which it
571 was previously attributed. However, there are some significant morphological links
572 between *Atractophora* and the Peyssonneliales. The tetrasporophyte of *Atractophora*
573 *hypnoides*, described by Crouan and Crouan (1859) as *Rhododiscus pulcherrimus*, was
574 placed provisionally in the Squamariaceae (= Peyssonneliaceae) by Denizot (1968).
575 The *Rhododiscus* phase of *Atractophora* consists of a compact disc with a
576 heterotrichous construction, in which prostrate filaments growing from a multiaxial
577 margin give rise to erect filaments (Fig. 5, a-f). Tetrasporangia are formed terminally
578 on the erect filaments, large, and regularly cruciately divided (Fig. 5, d-f), resembling
579 those of *Peyssonnelia* species (Maggs and Irvine 1983). Furthermore, during
580 development of male reproductive structures, members of the Peyssonneliaceae often
581 exhibit a uniaxial filamentous construction with whorls of periaxial filaments around
582 each “axial” cell (Kylin 1956, fig. 118B, Maggs and Irvine 1983, fig. 30). Post-
583 fertilization development in *Peyssonnelia* species reportedly involves the fusion of the
584 carpogonium with the hypogynous and subhypogynous cells of the carpogonial branch,
585 but the auxiliary cell is in a separate filament, i.e. nonprocarpic, and gonimoblasts arise
586 either from a diploidized auxiliary cell or directly from connecting filaments that form
587 expansive networks (Maggs and Irvine 1983, Dixon and Saunders 2013).

588 The question of whether the similarities between *Atractophora* and the
589 Peyssonneliales are sufficient to justify expanding the Peyssonneliales to include
590 *Atractophora* is a difficult one. Clearly, there are marked contrasts between
591 *Atractophora* and the Peyssonneliales, such as procarpic versus nonprocarpic
592 reproduction. The Peyssonneliales exhibits a consistent vegetative and reproductive
593 architecture such that we find it impossible to reconcile the assignment of *Atractophora*
594 to this order. We therefore propose placing the genus *Atractophora* in the
595 Atractophoraceae fam. nov., Atractophorales ord. nov.

596 Schils et al. (2003) noted similarities between the Naccariaceae and the
597 monotypic genus *Liagorothamnion*, described as an atypical member of the

598 Ceramiaceae (Huisman et al. 2000). These similarities include the formation of sterile
599 cell groups on the supporting cell and carpogonial branch cells. However, many key
600 features of its vegetative and post-fertilization development are closer to those of
601 *Atractophora* than to the rest of the Naccariaceae. In particular, the vegetative axis
602 consists of a narrow axial filament lacking the expanded “jacket” cells observed in the
603 Naccariaceae (Huisman et al. 2000, Schils et al. 2003). The formation in
604 *Liagorothamnion* of gonimoblasts from the fertilized carpogonium following fusion
605 with the supporting cell also contrasts with *Naccaria* and the rest of the Naccariaceae, in
606 which the carpogonium first fuses with the hypogynous cell (Kylin 1928, Hommersand
607 and Fredericq 1990). Based on this anatomical evidence we propose that
608 *Liagorothamnion* (for *Liagorothamnion mucooides* Huisman, D.L.Ballantine &
609 M.J.Wynne) be placed in the Atractophoraceae.

610 Lindstrom (1987) erected the family Acrosymphytaceae based mainly on the
611 terminal rather than intercalary position of the auxiliary cell for species of
612 *Acrosymphyton* versus the Dumontiaceae *sensu stricto*. Lindstrom (1987) commented
613 on similarities to the Calosiphoniaceae or Naccariaceae, but argued for a separate family
614 because members of the Calosiphoniaceae have intercalary auxiliary cells while those of
615 the Naccariaceae were considered procarpic in contrast to the terminal auxiliary cells
616 and nonprocarpy of the Acrosymphytaceae.

617 Tai et al. (2001) provided molecular evidence in support of the
618 Acrosymphytaceae as distinct from the Dumontiaceae and further suggested that this
619 family might not even be a member of the Gigartinales. Saunders et al. (2004)
620 expanded on that study and uncovered a strong association of the genus
621 *Schimmelmannia*, at that time assigned to the Gloiosiphoniaceae (Gigartinales), with the
622 Acrosymphytaceae. This was an interesting discovery because species of
623 *Schimmelmannia*, despite being procarpic, produce a terminal auxiliary cell as in the
624 Acrosymphytaceae and unlike the generitype of the Gloiosiphoniaceae (Kylin 1930).
625 Saunders et al. (2004) transferred *Schimmelmannia* to the Acrosymphytaceae despite
626 the respective procarpic versus nonprocarpic post-fertilization patterns, placing
627 taxonomic significance on the terminal auxiliary cells. The Acrosymphytaceae
628 (including *Schimmelmannia*) weakly resolved in a larger clade including the Ceramiales
629 (members of which also produce terminal auxiliary cells) and the Calosiphoniaceae.

630 Despite the previous molecular indications, Saunders et al. (2004) retained the
631 Acrosymphytaeae and Calosiphoniaceae in the Gigartinales arguing that formal
632 taxonomic proposals were premature. Subsequent molecular analyses by Withall and
633 Saunders (2006) were sufficiently robust to recognize a new order for *Acrosymphyton*
634 and *Schimmelmannia*, Acrosymphytales, solidly resolved as sister to the Ceramiales
635 with the Calosiphoniaceae as sister to the previous two orders. The Calosiphoniaceae
636 were considered *incertae sedis* pending study of the generitype *Calosiphonia* (Withall
637 and Saunders 2006). The Calosiphoniaceae remain a distinct lineage in our analyses
638 (Fig. 1); however, taxonomic proposals remain premature as we lack molecular data for
639 both the type of *Schmitzia* and, more importantly, *Calosiphonia*.

640 The resolution of our new Tasmanian species *Acrothesaurum gemellifilum*
641 within the Acrosymphytales prompted us to consider family-level taxonomy.
642 *Acrosymphyton* is highly distinctive from *Acrothesaurum* and *Schimmelmannia* as it is
643 characterized by carpogonial branches bearing pinnate laterals, production of primary
644 connecting filaments on presumed fertilization that first fuse with cells of the
645 carpogonial-branch laterals, which in turn issue lengthy septate secondary connecting
646 filaments that seek out distant (i.e., nonprocarpic) auxiliary cells terminating short,
647 unbranched “adventitious” filaments, diploidize them, and then continue on to effect
648 large numbers of further diploidizations (Sjöstedt 1926, Kraft 1981, fig. 1.1, Millar and
649 Kraft 1984, figs. 7-9, 15). *Schimmelmannia*, on the other hand, is procarpic with the
650 supporting cell bearing both the carpogonial and auxiliary-cell branches, the former
651 simple and not pinnate as in *Acrosymphyton* (Kylin 1930). Following fertilization in
652 *Schimmelmannia* the carpogonium typically undergoes one or two divisions (with one
653 exception; Ballantine et al. 2003), with one of the resulting cells fusing directly to the
654 auxiliary cell (Kylin 1930), again in stark contrast to *Acrosymphyton*. Our new
655 Tasmanian genus, *Acrothesaurum*, differs from both *Acrosymphyton* and
656 *Schimmelmannia* in that following fertilization the carpogonium fuses directly with an
657 auxiliary cell without intervening connecting filaments or connecting cells, respectively.
658 It is further unusual in blurring the lines between procarpy and nonprocarpy in that
659 auxiliary cells are diploidized both in the same and in separate branch systems by post-
660 fertilization carpogonia. To avoid paraphyly (Fig. 1; Table 1), and in consideration of
661 the significant anatomical differences for *Acrosymphyton* relative to *Acrothesaurum* and

662 *Schimmelmannia*, we have recognized the latter two at the family level in the
663 Acrosymphytales.

664 The blurring of the procarpic and nonprocarpic conditions in this family may
665 represent a transitional state from the procarpic Schimmelmanniaceae to the elaborate
666 nonprocarpy characteristic of the Acrosymphytaceae (Fig. 1). The sister relationship of
667 the Acrosymphytales to the procarpic Ceramiales, combined with the early divergence
668 of the procarpic Schimmelmanniaceae, render it parsimonious to conclude that procarpy
669 is ancestral to nonprocarpy in the Acrosymphytales. For this lineage at least, this
670 reverses the long-standing paradigm that nonprocarpy is an ancestral condition to
671 procarpy and that the Ceramiales are the apogee of red algal evolution (Kylin 1956).

672 *Acrothesaurum gemellifilum* is another novel addition to our knowledge of
673 Tasmanian algal biodiversity as it displays vegetative characters seemingly typical of
674 the Gloiosiphoniaceae (Gigartinales), a family heretofore unknown in Australia
675 (Womersley 1994). Molecular analyses, however, revealed an unexpected alliance with
676 the Acrosymphytales, a small order including species that classical morphologists
677 would not have been likely to classify correctly. Recognition of the Acrosymphytales
678 as presented here emphasizes the importance of the terminal auxiliary cell as a
679 diacritical marker among “gloiosiphonioid” taxa (Yeh and Yeh 2008, p. 337). The
680 affinities of the genera *Gloeophycus* and *Peleophycus* need consideration as both are
681 atypical members of the Gloiosiphoniaceae in being characterized by terminal auxiliary
682 cells.

683 *Gloeophycus* is lubricous in habit and lacks the pinnate carpogonial branch of
684 the Acrosymphytaceae (Lee and Yoo 1979). It is procarpic and in this regard more
685 reminiscent of the Acrothesauraceae and Schimmelmanniaceae, although more akin to
686 the latter (Kaneko et al. 1980). Pending much needed insights of molecular data this
687 genus is provisionally placed in the Schimmelmanniaceae, Acrosymphytales.

688 *Peleophycus* is a Hawaiian endemic monotypic genus (Abbott 1984). Limited
689 LSU data (664 bp) in GenBank (HQ421875) for *Peleophycus multiprocarpius*
690 I.A. Abbott solidly ally this genus to the Acrothesauraceae (not shown). Like
691 *Acrothesaurum*, *P. multiprocarpius* is lubricous, has similarly structured laterals
692 (Abbott 1984, figs 2, 7, 8), spermatangia (Abbott 1984, fig. 9), and
693 carpogonial/auxiliary-cell branches (Abbott 1984, figs. 5 and 6). It differs in the

694 relative simplicity of its rhizoidal cortication (Abbott 1984, fig. 4), which apparently
695 does not produce perpendicular corticating filaments, the division of presumably
696 fertilized carpogonia and the diploidization of auxiliary cells by a connecting cell
697 produced by a derivative cell of the divided carpogonium, and an apparent lack of the
698 stout tubular gonimoblasts that arise from proximal auxiliary-cell surfaces to connect to
699 subtending central-axial cells. Whereas *Peleophycus* was reported as strictly procarpic
700 (Abbott 1984, p. 330), the possibility that carpogonia can diploidize auxiliary cells in
701 separate branch systems as noted here for *Acrothesaurum* should be explored.

702

703 **Acknowledgements**

704 All of the collectors (listed with the accessions for the COI-5P data in GenBank) are
705 thanked for their contributions to this study, as is T. Moore for generating most of the
706 sequence data. This research was supported through funding to GWS from the
707 Canadian Barcode of Life Network from Genome Canada through the Ontario
708 Genomics Institute, Natural Sciences and Engineering Research Council of Canada and
709 other sponsors listed at www.BOLNET.ca. Additional support to GWS was provided
710 by the Canada Research Chair Program, the Canada Foundation for Innovation and the
711 New Brunswick Innovation Foundation, as well as NSF through the RedToL project
712 (DEB 0937975).

713

714 Abbott, I. A. 1984. *Peleophycus multiprocarpium* gen. et sp. nov. (Gloiosiphoniaceae,
715 Rhodophyta). *Pac. Sci.* 38:324-332.

716 Agardh, J. G. 1863. *Species genera et ordines algarum, seu descriptiones succinctae*
717 *specierum, generum et ordinum, quibus algarum regnum constituitur. Volumen*
718 *secundum: algas florideas complectens*. C.W.K. Glerup, Lundae (Lund), Part 2,
719 fasc. 3. pp. 787-1138, 1158-1291.

720 Agardh, J. G. 1876. *Species, Genera et Ordines Algarum*. T.O. Weigel, Leipzig, Vol. 3,
721 fasc. 1. pp. viii-724.

722 Ballantine, D. L., Garcia, M., Gomez, S. & Wynne, M. J. 2003. *Schimmelmannia*
723 *venezuelensis* sp. nov. (Gloiosiphoniaceae, Rhodophyta) from Venezuela. *Bot. Mar.*
724 46:450-455.

- 725 Chapman, V. J. 1979. Issue 4: Gigartinales. In Chapman, V. J. [Ed.] *The marine algae*
726 *of New Zealand. Part III. Rhodophyceae*. Cramer, Lehre, pp. 279-506.
- 727 Chihara, M. & Yoshizaki, M. 1972. Bonnemaisioniaceae: their gonimoblast
728 development, life history and systematics. In Abbott, I. A. & Kurogi, M. [Eds.]
729 *Contributions to the Systematics of Benthic Marine Algae of the North Pacific*. Jap.
730 Soc. Phycol., Kobe, Japan, pp. 243-251.
- 731 Crouan, P. L. & Crouan, H. M. 1848. Études sur l'organisation, la fructification et la
732 classification du *Fucus wiggghii* de Turner et de Smith, et de l'*Atractophora*
733 *hypnoides*. *Ann. Sci. Nat. Bot.* 10:361-376.
- 734 Crouan, P. L. & Crouan, H. M. 1859. Notice sur quelques espèce et genres nouveaux
735 d'algues marines de la Rade de Brest. *Ann. Sci. Nat. Bot. Quat. série* 12:288-292,
736 pls. 21.
- 737 Denizot, M. 1968. *Les algues floridées encroustantes (à l'exclusion des corallinacées)*.
738 PhD thesis, Université de Paris, Faculté des sciences, Paris.
- 739 Dixon, P. S. & Irvine, L. M. 1977. *Seaweeds of the British Isles. Vol. 1. Rhodophyta,*
740 *Part 1. Introduction, Nemaliales, Gigartinales*. British Museum (Natural History),
741 London, England.
- 742 Dixon, K. R. & Saunders, G. W. 2013. DNA barcoding and phylogenetics of
743 *Ramicrusta* and *Incendia* gen. nov., two early diverging lineages of the
744 Peyssonneliaceae (Rhodophyta). *Phycologia* 52:82-108.
- 745 Fan, K. C. 1961. Morphological studies of the Gelidiales. *Univ. Calif. Publ. Bot.* 32:[i-
746 iv], 315-368, 15 figs, pls. 33-46.
- 747 Feldmann, J. & Feldmann, G. 1942. Recherches sur les Bonnemaisioniacées et leur
748 alternance de générations. *Ann. Sci. Nat. Bot. Ser.* 11, 3: 75-175.
- 749 Gavio, B., Hickerson, E., & Fredericq, S. 2005. *Platoma chrysymenioides* sp. nov.
750 (Schizymeniaceae), and *Sebdenia integra* sp. nov. (Sebdeniaceae), two new red
751 algal species from the northwestern Gulf of Mexico, with a phylogenetic
752 assessment of the Cryptonemiales complex (Rhodophyta). *Gulf Mex. Sci.* 1:38-57.
- 753 Guiry, M. D. & Cunningham, E. C. 1984. Photoperiodic and temperature responses in
754 the reproduction of north-eastern Atlantic *Gigartina acicularis* (Rhodophyta:
755 Gigartinales). *Phycologia* 23:357-367.

- 756 Guiry, M. D. & Guiry, G. M. 2015. AlgaeBase. World-wide electronic publication,
757 National University of Ireland, Galway. <http://www.algaebase.org> (searched on 26
758 October, 2015).
- 759 Harper, J. T. & Saunders, G. W. 2001. Molecular systematics of the Florideophyceae
760 (Rhodophyta) using nuclear large- and small-subunit rDNA sequence data. *J.*
761 *Phycol.* 37:1073-1082.
- 762 Hommersand, M. H. & Fredericq, S. 1990. Sexual reproduction and cystocarp
763 development. In K. M. Cole and R. G. Sheath [Eds.], *Biology of the red algae*.
764 Cambridge University Press, Cambridge, pp. 305-345.
- 765 Huisman J. M., Ballantine D. L. & Wynne J. M. 2000. *Liagorothamnion mucoides* gen.
766 et sp. nov. (Ceramiaceae, Rhodophyta) from the Caribbean Sea. *Phycologia* 39:507-
767 516.
- 768 Kaneko, T., Matsuyama, K. & Yamada, I. 1980. On *Gloeophycus koreanum* I.K. Lee &
769 Yoo (Rhodophyta, Gloiosiphoniaceae) in Hokkaido. *Jap. J. Phycol.* 28:97-104.
- 770 Kearse, M., Moir, R., Wilson, A., Stones-Havas, S., Cheung, M., Sturrock, S., Buxton,
771 S., Cooper, A., Markowitz, S., Duran, C., Thierer, T., Ashton, B., Mentjies, P. &
772 Drummond, A. 2012. Geneious Basic: an integrated and extendable desktop
773 software platform for the organization and analysis of sequence data. *Bioinformatics*
774 28:1647-1649
- 775 Kraft, G. T. 1981. Rhodophyta: morphology and classification. In Lobban, C.S. &
776 Wynne, M.J. [Eds.] *Biology of Seaweeds*. Blackwell Scientific Publications,
777 London, pp. 6-51.
- 778 Kravesky, D. M., Norris, J. N., Gabrielson, P. W., Gabriel, D. & Fredericq, S. 2009. A
779 new order of red algae based on the Peyssoneliaceae, with an evaluation of the
780 ordinal classification of the Florideophyceae (Rhodophyta). *Proc. Biol. Soc. Wash.*
781 122:364-391.
- 782 Kützing, F. T. 1849. Diagnosen und Bemerkungen zu neuen oder kritischen Algen. *Bot.*
783 *Zeitung* 5:1-5, 22-25, 33-38, 52-55, 164-167, 177-180, 193-198, 219-223.
- 784 Kylin, H. 1928. Entwicklungsgeschichtliche Florideenstudien. *Lunds Univ. Arsskr. N.F.*
785 *Avd. 2* 84:1-127.
- 786 Kylin, H. 1930. Über die Entwicklungsgeschichte der Florideen. *Lunds Univ. Arsskr.*
787 *N.F. Avd. 2* 26:1-104

- 788 Kylin, H. 1932. Die Florideenordnung Gigartinales. *Acta Univ. Lund.* 28:1-88, 22 figs,
789 pls. 28.
- 790 Kylin, H. 1956. *Die Gattungen der Rhodophyceen.* C.W.K. Gleerups, Lund, pp. i-xv, 1-
791 673.
- 792 Lanfear, R., Calcott, B., Ho, S. Y. W. & Guindon, S. 2012. PartitionFinder: Combined
793 Selection of Partitioning Schemes and Substitution Models for Phylogenetic
794 Analyses. *Mol. Biol. Evol.* 29(6):1695-1701.
- 795 Le Gall, L. & Saunders, G. W. 2007. A nuclear phylogeny of the Florideophyceae
796 (Rhodophyta) inferred from combined EF2, small subunit and large subunit
797 ribosomal DNA: Establishing the new red algal subclass Corallinophycidae. *Mol.*
798 *Phyl. Evol.* 43:1118-1130.
- 799 Lee, I. K. & Yoo, S. A. 1979. *Gloeophycus koreanum* gen. et sp. nov. (Rhodophyta,
800 Gloiosiphoniaceae) from Korea. *Phycologia* 18:347-354.
- 801 Lindstrom, S. C. 1987. Acrosymphytaceae, a new family in the order Gigartinales *sensu*
802 *lato* (Rhodophyta). *Taxon* 36:50-53.
- 803 Maggs, C. A. 1988. Intraspecific life history variability in the Florideophycidae
804 (Rhodophyta). *Bot. Mar.* 31:465-490.
- 805 Maggs, C. A. 1989. *Erythrodermis allenii* Batters in the life history of *Phyllophora*
806 *traillii* Holmes ex Batters (Phylloporaceae, Rhodophyta). *Phycologia* 28:305-317.
- 807 Maggs, C. A. & Irvine, L. M. 1983. *Peyssonnelia immersa* sp. nov. (Cryptonemiales,
808 Rhodophyta) from the British Isles and France, with a survey of infrageneric
809 classification. *Br. Phycol. J.* 18:219-238.
- 810 Millar, A. J. K. & Kraft, G. T. 1984. The red algal genus *Acrosymphyton*
811 (Dumontiaceae, Cryptonemiales) in Australia. *Phycologia* 23:135-145.
- 812 Oltmanns, F. 1904. *Morphologie und Biologie der Algen.* Erster Band. Spezieller Teil.
813 Verlag von Gustav Fischer, Jena, pp. [i]-vi, [1]-733, 467 figs, 3 pls.
- 814 Papenfuss, G. F. 1966. A review of the present system of classification of the
815 Florideophycidae. *Phycologia* 5:247-255.
- 816 Pond, S. L. K., Frost, S. D. W. & Muse, S. V. 2005. "HyPhy: hypothesis testing using
817 phylogenies". *Bioinformatics* 21:676-679.
- 818 Pueschel, C. M. & Cole, K. M. 1982. Rhodophycean pit plugs: An ultrastructural survey
819 with taxonomic implications. *Am. J. Bot.* 69:703-720.

- 820 Robins, P. A. 1990. The morphology of *Catenellopsis* (Catenellopsidaceae, fam. nov.;
821 Rhodophycota). *Aust. Syst. Bot.* 3:689-699.
- 822 Saunders, G. W. & Bailey, J. C. 1997. Phylogenesis of pit-plug associated features in
823 the Rhodophyta: inferences from molecular systematic data. *Can. J. Bot.* 75:1436-
824 1447.
- 825 Saunders, G. W. & Bailey, J. C. 1999. Molecular systematic analyses indicate that the
826 enigmatic *Apophlaea* is a member of the Hildenbrandiales (Rhodophyta,
827 Florideophycidae). *J. Phycol.* 35:171-175.
- 828 Saunders, G. W., Chiovitti, A. & Kraft, G. T. 2004. Small-subunit rDNA sequences
829 from representatives of selected families of the Gigartinales and Rhodymeniales
830 (Rhodophyta). 3. Delineating the Gigartinales *sensu stricto*. *Can. J. Bot.* 82:43-74.
- 831 Saunders, G. W. & Hommersand, M. 2004. Assessing red algal supraordinal diversity
832 and taxonomy in the context of contemporary systematic data. *Amer. J. Bot.*
833 91:1494-1507.
- 834 Saunders, G. W. & McDevit, D. C. 2012. Methods for DNA barcoding photosynthetic
835 protists emphasizing the macroalgae and diatoms. *Methods Mol. Biol.* 858:207-222.
- 836 Saunders, G. W. & Moore, T. E. 2013. Refinements for the amplification and
837 sequencing of red algal DNA barcode and RedToL phylogenetic markers: a
838 summary of current primers, profiles and strategies. *Algae* 28:31-43.
- 839 Schils, T., De Clerck, O. & Coppejans, E. 2003. The red algal genus *Reticulocaulis*
840 from the Arabian Sea, including *R. obpyriformis* sp. nov., with comments on the
841 family Naccariaceae. *Phycologia* 42:44-55.
- 842 Schmitz, F. & Hauptfleisch, P. 1897. Gelidiaceae. In Engler, A. & Prantl, K. [Eds.] *Die*
843 *natürlichen Pflanzenfamilien nebst ihren Gattungen und wichtigeren Arten*
844 *insbesondere den Nutzpflanzen unter Mitwirkung zahlreicher hervorragender*
845 *Fachgelehrten, Teil 1, Abteilung 2*. Verlag von Wilhelm Engelmann, Leipzig, pp.
846 340-349.
- 847 Sjöstedt, L. G. 1926. Floridean studies. *Lunds Univ. Arsskr. N.F. Avd. 2* 22:1-95.
- 848 Stamatakis, A. 2014. RAxML Version 8: A tool for phylogenetic analysis and post-
849 analysis of large phylogenies. *Bioinformatics* 30:312-1313.

- 850 Tai, V., Lindstrom, S. C. & Saunders, G. W. 2001. Phylogeny of the Dumontiaceae
851 (Gigartinales, Rhodophyta) and associated families based on SSU rDNA and
852 internal transcribed spacer sequence data. *J. Phycol.* 37:184-196.
- 853 Verbruggen, H., Maggs, C. A., Saunders, G. W., Le Gall, L., Yoon, H. -S. & De Clerck,
854 O. 2010. Data mining approach identifies research priorities and data requirements
855 for resolving the red algal tree of life. *BMC Evol. Biol.* 10:16
856 (<http://www.biomedcentral.com/1471-2148/10/16>).
- 857 Verbruggen, H. 2012. SiteStripper v.1.01. GNU General Public
858 License. <http://www.phycoweb.net/software/SiteStripper/index.html>
- 859 Withall, R. D. & Saunders, G. W. 2006. Combining small and large subunit ribosomal
860 DNA genes to resolve relationships among orders of the Rhodymeniophycidae
861 (Rhodophyta): recognition of the Acrosymphytales ord. nov. and Sebdeniales ord.
862 nov. *Eur. J. Phycol.* 41:379-394.
- 863 Wittmann, W. 1965. Aceto-iron-haematoxylin-chloral hydrate for chromosome staining.
864 *Stain Technol.* 40:161-164.
- 865 Womersley, H. B. S. 1994. *The Marine Benthic Flora of Southern Australia, Part IIIA*.
866 Australian Biological Resources Study & the State Herbarium of South Australia,
867 Adelaide & Canberra.
- 868 Womersley, H. B. S. 1996. *The marine benthic flora of southern Australia - Part IIIB -*
869 *Gracilariales, Rhodymeniales, Corallinales and Bonnemaisoniales*. Australian
870 Biological Resources Study & the State Herbarium of South Australia, Adelaide &
871 Canberra.
- 872 Wróbel, B. 2008. Statistical measures of uncertainty for branches in phylogenetic trees
873 inferred from molecular sequences by using model-based methods. *J. Appl. Genet.*
874 49:49-67.
- 875 Yang, E. C. et al. 2015. Highly conserved mitochondrial genomes among multicellular
876 red algae of the Florideophyceae. *Genome Biol. Evol.* 7:2394-2406.
- 877 Yeh, W. J. & Yeh, C. C. 2008. *Schimmelmannia formosana* sp. nov.
878 (Acrosymphytaceae, Rhodophyta) from Taiwan. *Phycologia* 47:337-345.
- 879 Yoon, H., Muller, K. M., Sheath, R. G., Ott, F. D. & Bhattacharya, D. 2006. Defining
880 the major lineages of red algae (Rhodophyta). *J. Phycol.* 42:482-492.

881 Zerlang, O. E. 1889. Entwicklungsgeschichtliche Untersuchungen über die Florideen-
 882 Gattungen Wrangelia und Naccaria. *Flora (Jena)* 72:371-407.

883

884 TABLE 1. Bayesian posterior probabilities and RAxML bootstrap values corresponding
 885 to the nodes in Figure 1. Results are included for the original alignment without
 886 PartitionFinder partitioning schemes (noPF; i.e., fully partitioned) and with
 887 PartitionFinder (PF), as well as maximum likelihood bootstrap values for the “stripped”
 888 alignments without PartitionFinder partition schemes. Dashes (-) indicate nodal support
 889 below 50%. n/a indicates a node that was not resolved.

890

Nodes	Full alignment									
	Bayes		ML		Percentage of stripping for ML no PF analyses					
	no PF	PF	no PF	PF	5%	10%	15%	20%	25%	
A	1	0.97	100	100	100	100	100	100	100	
B	0.99	0.97	93	92	90	94	90	68	55	
C	0.94	0.90	66	66	65	81	50	-	n/a	
D	0.99	0.97	96	97	97	96	71	61	n/a	
E	1	0.95	89	91	97	79	n/a	54	n/a	
F	0.99	0.90	52	49	54	76	73	80	-	
G	0.99	1	65	66	67	76	71	-	-	
H	0.99	0.99	77	77	75	92	87	61	55	
I	0.99	0.97	89	89	87	90	80	80	-	
J	0.99	0.97	97	96	96	99	95	86	55	
K	0.51	n/a	n/a	n/a	n/a	n/a	n/a	60	-	
L	0.89	0.78	-	-	-	-	53	51	n/a	
M	0.99	0.97	100	100	100	100	n/a	100	100	
N	0.98	0.95	66	66	76	71	n/a	-	n/a	
a	0.99	0.99	96	98	98	97	99	100	98	
b	0.99	1	100	100	100	100	100	100	100	

c	0.99	1	80	81	85	81	80	50	53
d	0.95	0.94	68	69	75	81	83	68	58
e	1	1	100	100	100	100	100	100	89
f	1	1	100	100	100	100	100	100	100
g	1	1	100	100	100	100	100	100	100
h	0.99	1	100	100	100	100	100	100	99
i	0.99	1	100	100	100	100	100	100	100
j	1	1	100	100	100	100	100	100	100
k	0.99	0.98	100	100	100	100	100	100	100
m	0.99	0.97	64	64	77	70	55	67	61

891

892 **Figure legends**

893

894 Fig. 1. Bayesian phylogeny for multigene alignment analyzed with full partitioning.
 895 Letters at nodes refer to respective support values in Table 1. New taxa in bold type.
 896 The outgroup Corallinophycidae have been cropped from the figure to facilitate
 897 presentation. Scale indicates substitutions per site.

898

899 Fig. 2. Specimen CO00288 from the brothers Crouan herbarium housed at the Muséum
 900 National d'Histoire Naturelle - Marinarium de Concarneau (CO) is here designated as
 901 the lectotype of *Atractophora hypnoides*.

902

903 Fig. 3a-m. Vegetative and reproductive structures of *Atractophora hypnoides*
 904 gametophytes in culture. The culture was isolated from tetraspores of field-collected
 905 *Rhododiscus pulcherrimus*. [Abbreviations: ax, axial cell; b, first (basal) carpogonial
 906 branch cell; c, carpogonium; cs, carposporangium; f, fusion cell; g, gonimoblast cell; gi,
 907 gonimoblast initial; h/hy, hypogynous cell; l, l1-l4, lateral cells of carpogonial branch; s,
 908 spermatangium; sm, spermatangial mother cell; sp, spermatium; su, supporting cell; tr,
 909 trichogyne.]

910 a. Uniaxial erect axis of *A. hypnoides* 18 d after inoculation of tetraspores, showing
 911 distichous branching pattern.

- 912 b. Erect axes after 29 d in culture, developing cruciate arrangement of whorl branchlets.
913 c. Apex of thallus after 46 d, showing transverse apical cell division, repositioning of
914 whorls around axial cells by elongation of axial cells, and terminal hair (arrow).
915 d. Cortication of axis (at 90 d) by downgrowing rhizoidal filaments produced by basal
916 cells of whorl branchlets (shaded).
917 e. Tufts of spermatangial mother cells bearing spermatangia after 46 d.
918 f-i. Stages of development of carpogonial branch.
919 j. Diagram of structure of mature carpogonial branch showing tufts of small "nutritive"
920 cells on the hypogynous cell, first carpogonial branch cell, and fourth lateral cell.
921 k. Carpogonial branch after fertilization, with spermatium attached to trichogyne.
922 Carpogonium and hypogynous cell appear to have fused; protuberance has developed
923 from supporting cell, to which lateral cell (l) is attached.
924 l. First carpogonial branch cell has apparently been included in fusion structure formed
925 by carpogonium, hypogynous cell and supporting cell, which has produced branching
926 gonimoblast filaments.
927 m. Gonimoblast filaments of mature carposporophyte, bearing terminal carposporangia,
928 after 95 d in culture.
929 Scale bars represent: a, b, 50 μm ; c, d, i, 20 μm ; e-h, j-m, 25 μm .

930

931 Fig. 4a-i. Reproductive structures of *A. hypnoides* gametophytes in culture.

932 [Abbreviations as for Fig. 3.]

- 933 a. Thallus apex bearing tufts of spermatangial branches (arrows).
934 b. Spermatangial mother cells giving rise to spermatangia.
935 c. Thallus with spermatangial tufts and mature carpogonial branch (arrow) with long
936 trichogyne and numerous attached and unattached spherical spermatia.
937 d. Young carpogonial branch with developing trichogyne.
938 e. Mature carpogonial branch showing 8-celled structure.
939 f, g. Post-fertilization development, with interpretation of complex structure drawn in
940 multiple focal planes. Carpogonium has fused with supporting cell, still attached to
941 axial cell (large arrow) to form fusion cell (shaded); gonimoblast initial and
942 gonimoblast filaments produced from carpogonial end of fusion cell (shown in f).
943 Second fusion cell consisting of hypogynous cell and first carpogonial branch cell (lies

944 over carpogonium); third fusion cell formed by lateral cells 2 and 4; three groups of
945 small nutritive cells (nut; small arrow) attached to these fusion cells.

946 h. Fusion cell (large arrow) with group of small nutritive cells (small arrow indicates
947 one cell).

948 i. Branching gonimoblast filaments with terminal cells developing into carposporangia.
949 Scale bars represent: a, 100 μm ; b, d, 5 μm ; c, 20 μm ; e-i, 10 μm .

950

951 Fig. 5a-f. Vegetative and reproductive structures of *Atractophora hypnoides*
952 tetrasporophytes in culture.

953 a. Poorly attached spore (left) produced long filament that by lateral branching formed a
954 disc after 31 d.

955 b. Radial vertical section of crust (at 102 d), showing origin of erect filaments from
956 basal layer cells, and elongated apical cells.

957 c. Stained crust from below. Polyflabellate pattern formed by cessation of growth of
958 most filaments soon after branching.

959 d. Radial vertical sections of crust showing origin of two erect filaments from long basal
960 layer cells, and pigmented apical cells (shaded) that develop into tetrasporangia (t)
961 following transfer to short daylengths (8 h).

962 e. Surface view of crust with mature tetrasporangia; patchy appearance results from
963 discharge of spores.

964 f. Vertical section through field-collected tetrasporophyte (as *Rhododiscus*
965 *pulcherrimus*) with developing and mature tetrasporangia.
966 Scale bars represent: a, 50 μm ; b, d, 20 μm ; c, e, f, 25 μm .

967

968 Fig. 6a-j. *Acrothesaurum gemellifilum* vegetative and spermatangial features of
969 holotype (GWS016355).

970 a. Slide-mounted fragment serving as holotype.

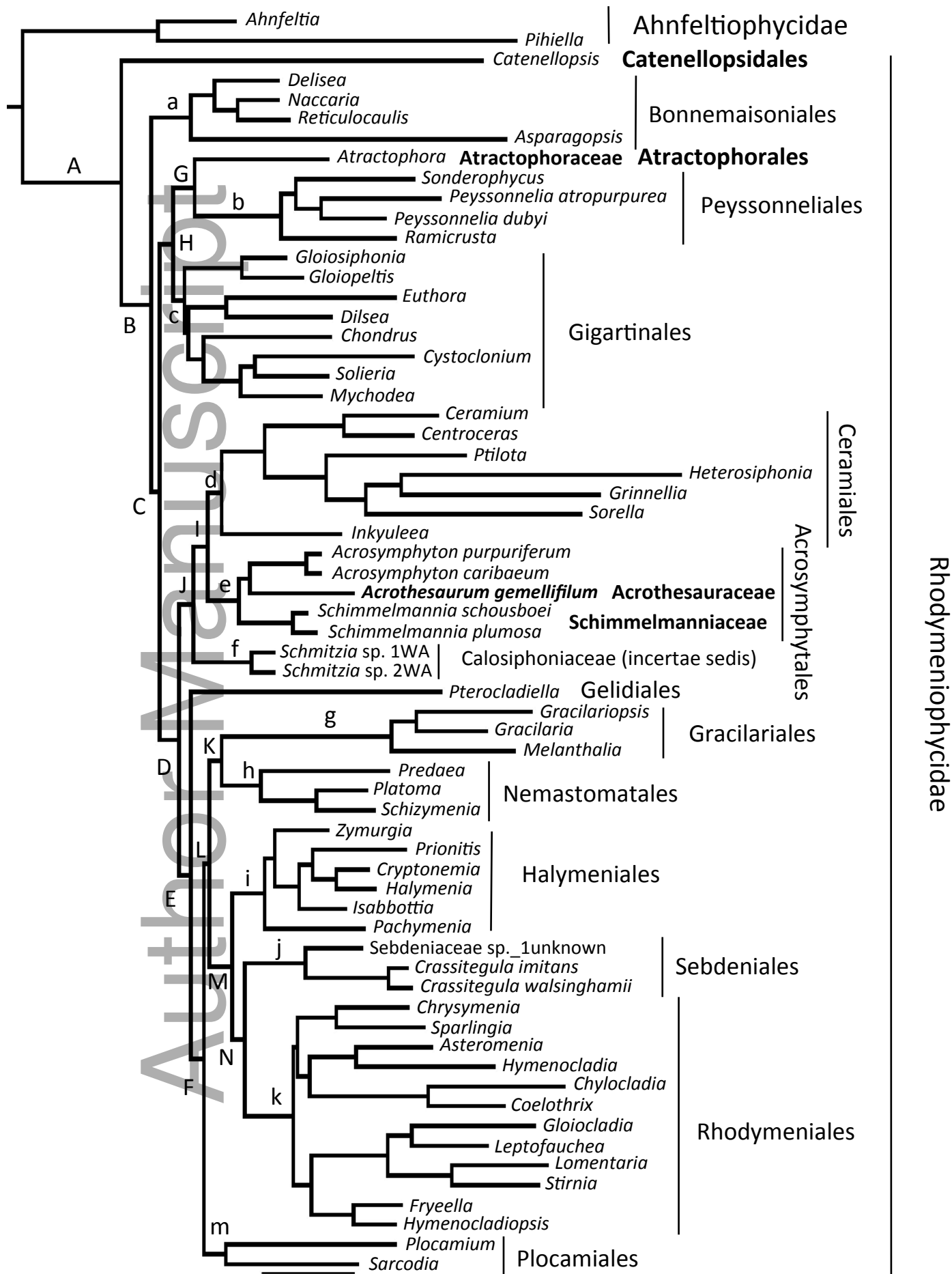
971 b. Habit of entire specimen from which holotype slide was prepared.

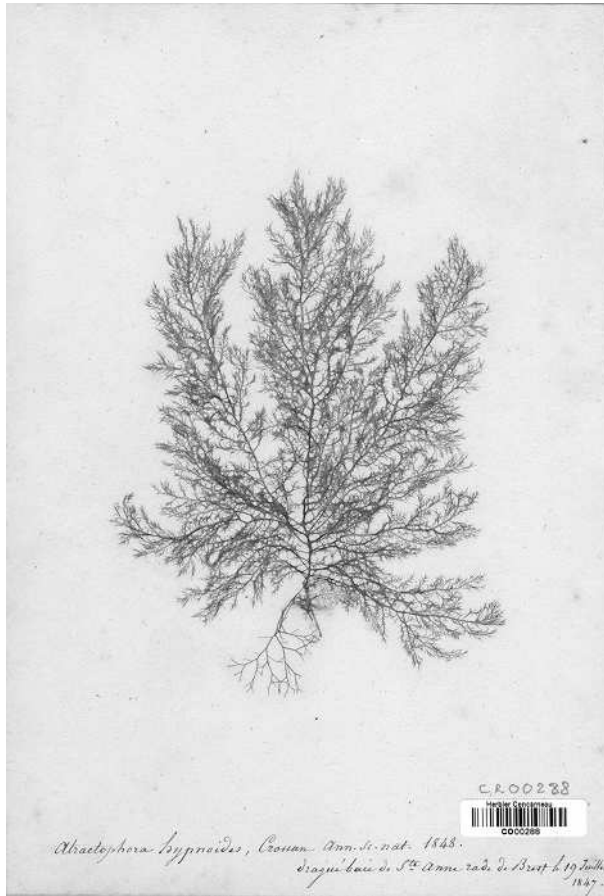
972 c. Gradually tapering tips of indeterminate laterals, with higher-order laterals (arrows)
973 arising from epi-periaxial cells of whorl branchlets.

974 d. Whorl laterals borne on periaxial cells ringing distal poles of central-axial cells;
975 higher-order lateral (arrowhead) growing from epi-periaxial cell (arrow).

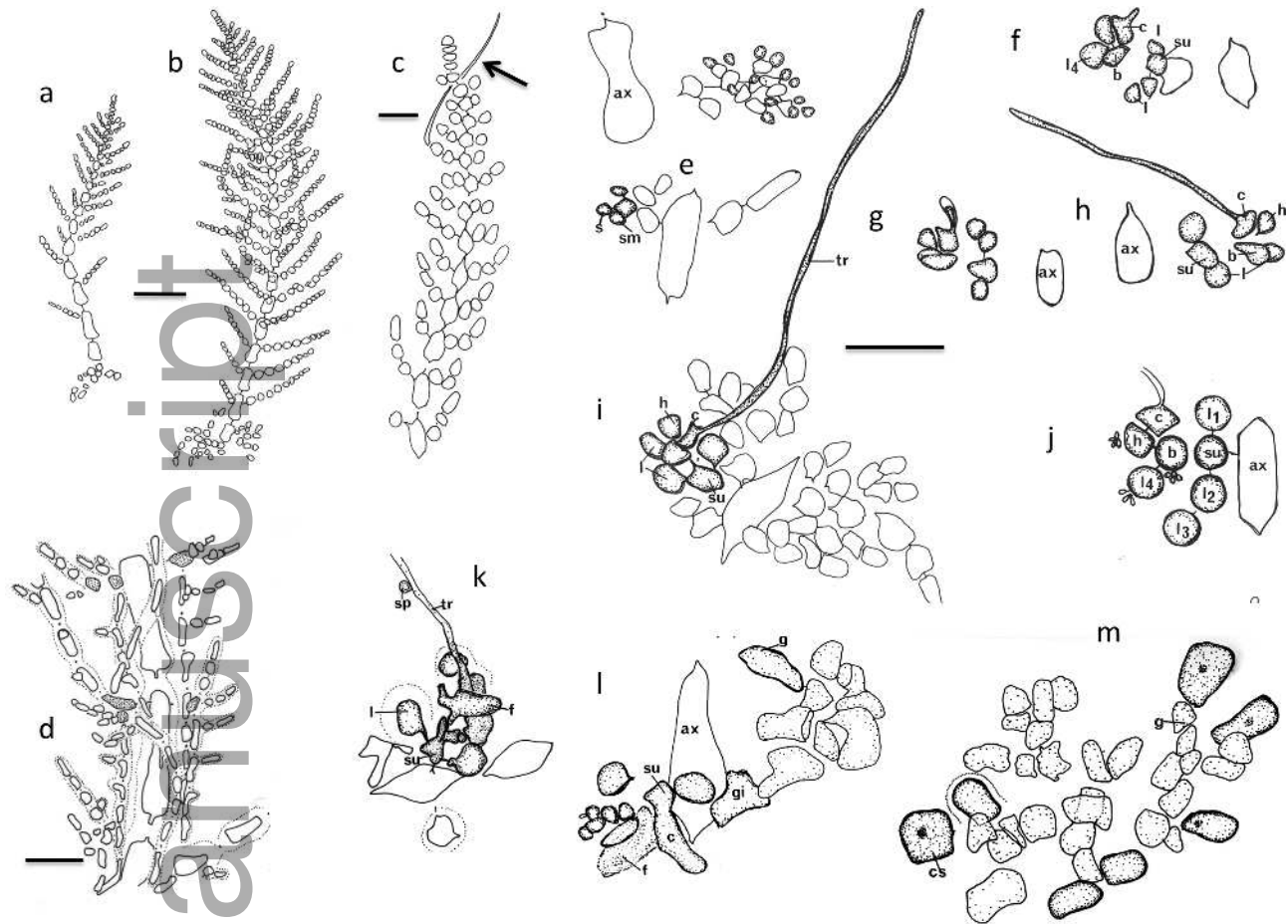
- 976 e. Apical cells of whorl-laterals that project into vegetative hairs (arrows).
977 f. Rhizoids initiated basipetally from periaxial cells that also bear carpogonial (arrow)
978 and auxiliary-cell (arrowhead) branches.
979 g. Basipetally growing rhizoids (arrowheads) producing lateral branches.
980 h. Complete internodal cover of central-axial cells by perpendicular determinate laterals
981 borne on rhizoidal filaments.
982 i. Whorl lateral of monoecious gametophyte with spermatangia borne singly
983 (arrowheads) or in multiples of two or three (double arrowheads) formed terminally or
984 subterminally, with an auxiliary-cell branch (arrow) directed basipetally from a
985 periaxial cell.
986 j. Cross-section of a gametophyte axis with terminal spermatangia on whorl laterals
987 borne on the four periaxial cells (arrowheads) surrounding the central-axial filament.
988
- 989 Fig. 7a-h. *Acrothesaurum gemellifilum* features of pre- and presumably post-
990 fertilization events (GWS016355). (Designations “a”, “b”, “ac” are basal, epibasal and
991 auxiliary cells, respectively; designations “1”, “2”, “3”, “cp” are basal, epibasal,
992 hypogynous cells and carpogonia, respectively. “sc” = supporting cell of carpogonial
993 and/or auxiliary-cell filaments.)
- 994 a. Periaxial and epi-periaxial (double arrowheads) cells bearing numerous auxiliary-cell
995 branches (arrowheads) and an immature carpogonial branch with rudimentary
996 trichogyne (arrow).
997 b. Periaxial and epi-periaxial cells bearing auxiliary-cell (arrowheads) and carpogonial
998 branches, trichogyne of one (arrow) apparently breaking down and leaving hypogynous
999 cell the size and position of an auxiliary cell.
1000 c. Terminal auxiliary cells (ac) and three carpogonial branches with early trichogynes
1001 (arrows).
1002 d. An anomalous five-celled carpogonial branch, carpogonium bearing a long sinuous
1003 trichogyne (arrow).
1004 e. Carpogonial branch with adjacent auxiliary cells (ac), trichogyne (arrow) extending
1005 to whorl surface and apparently bearing attached spermatium (arrowhead).
1006 f. Attachment of carpogonium to auxiliary cell (arrowhead) of sibling filament on
1007 supporting cell (sc) and cutting off of single gonimoblast initial (1' gbl).

1008 g. Three-celled stage of early gonimoblast (gbl) following procarpic fusion of
1009 carpogonium and auxiliary cell (arrow).
1010 h. As first gonimolobe matures, two basally directed arms of unknown function grow
1011 from extended auxiliary cell (ac).
1012
1013 Fig. 8a-f. *Acrothesarum gemellifilum* gonimoblast and carposporophyte features
1014 (GWS016355). (Photo annotations as in Fig. 7.)
1015 a. Fused carpogonia (arrow) and auxiliary cell (ac), latter viewed end-on and stoutly
1016 connected to gonimoblast initial (gi), which subtends early first gonimolobe.
1017 b, c. Diploidized auxiliary cells seen side-on (ac), cells eccentrically swollen and
1018 bearing early (5b) and mid (5c) primary gonimolobes.
1019 d. Terminal fusion of two auxiliary-cell arms (arrows) to adjacent central-axial cells
1020 (arrowheads).
1021 e. Mature primary gonimolobe on auxiliary cell (arrow) that has issued two inwardly
1022 growing arms (arrowheads) that are yet to fuse with central-axial cells.
1023 f. Mature carposporophyte consisting of three gonimolobes (gl-1, -2, -3) of successively
1024 maturing crops of carposporangia.
1025
1026 Supplementary Material
1027 Fig. S1. An alternative topology generated by neighbor-joining with the HKY model to
1028 assess the effect of the starting tree on our SiteStripper analyses.
1029 Table S1. A list of the taxa used in this study with the corresponding GenBank
1030 accessions for the five genes used in phylogenetic analyses.

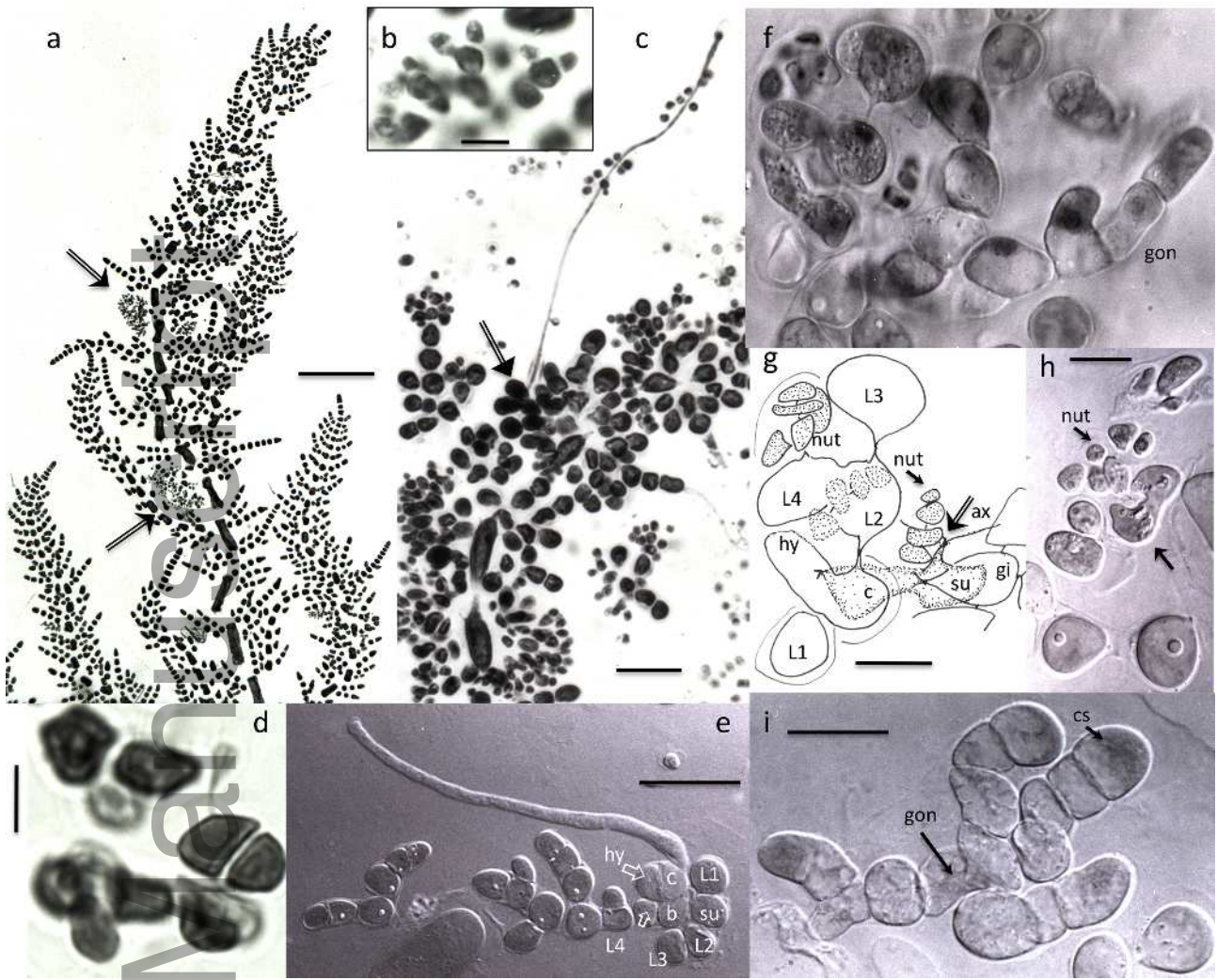




jpy_12426-16-002_f2.tif

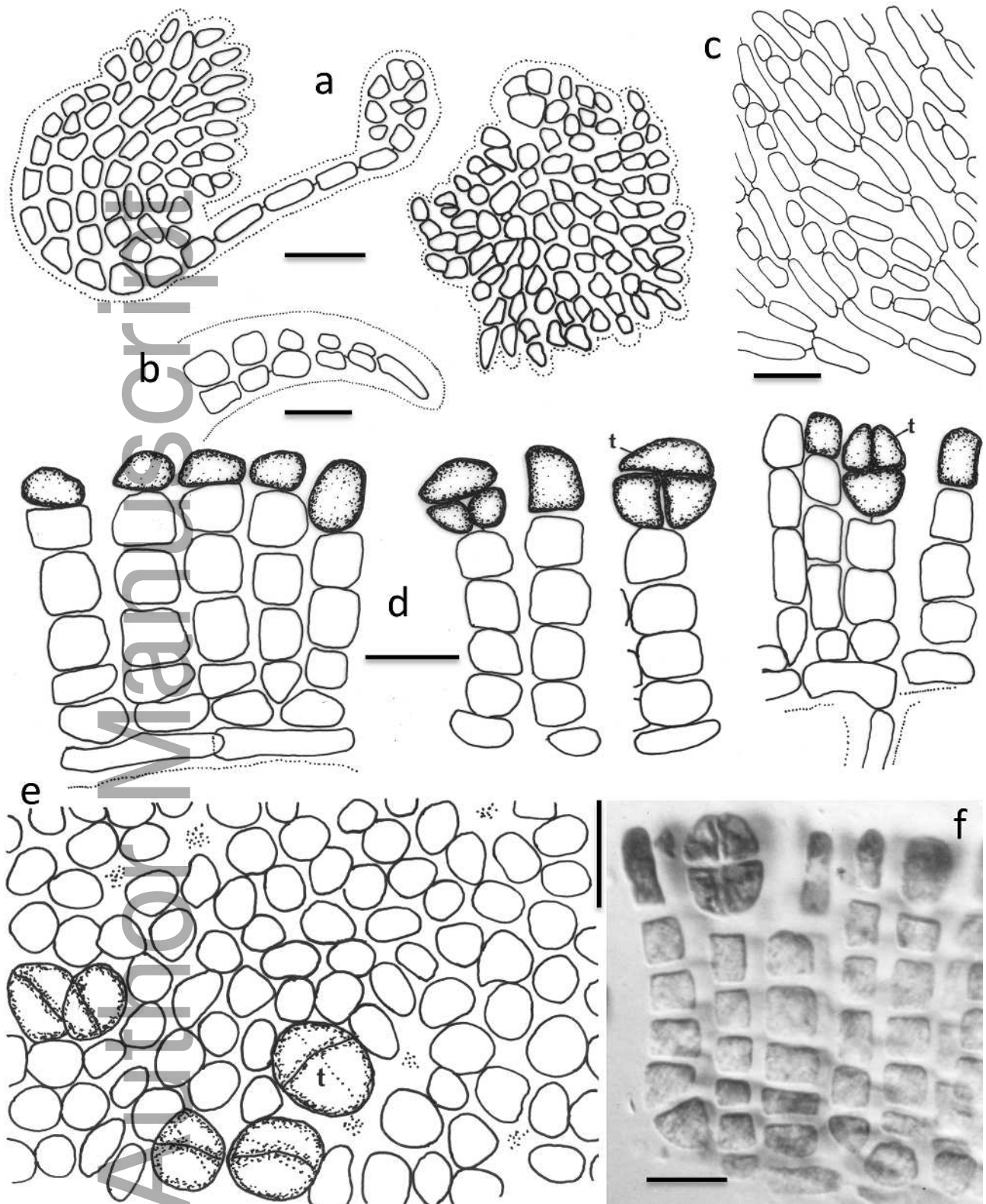


jpg_12426-16-002_f3.tif

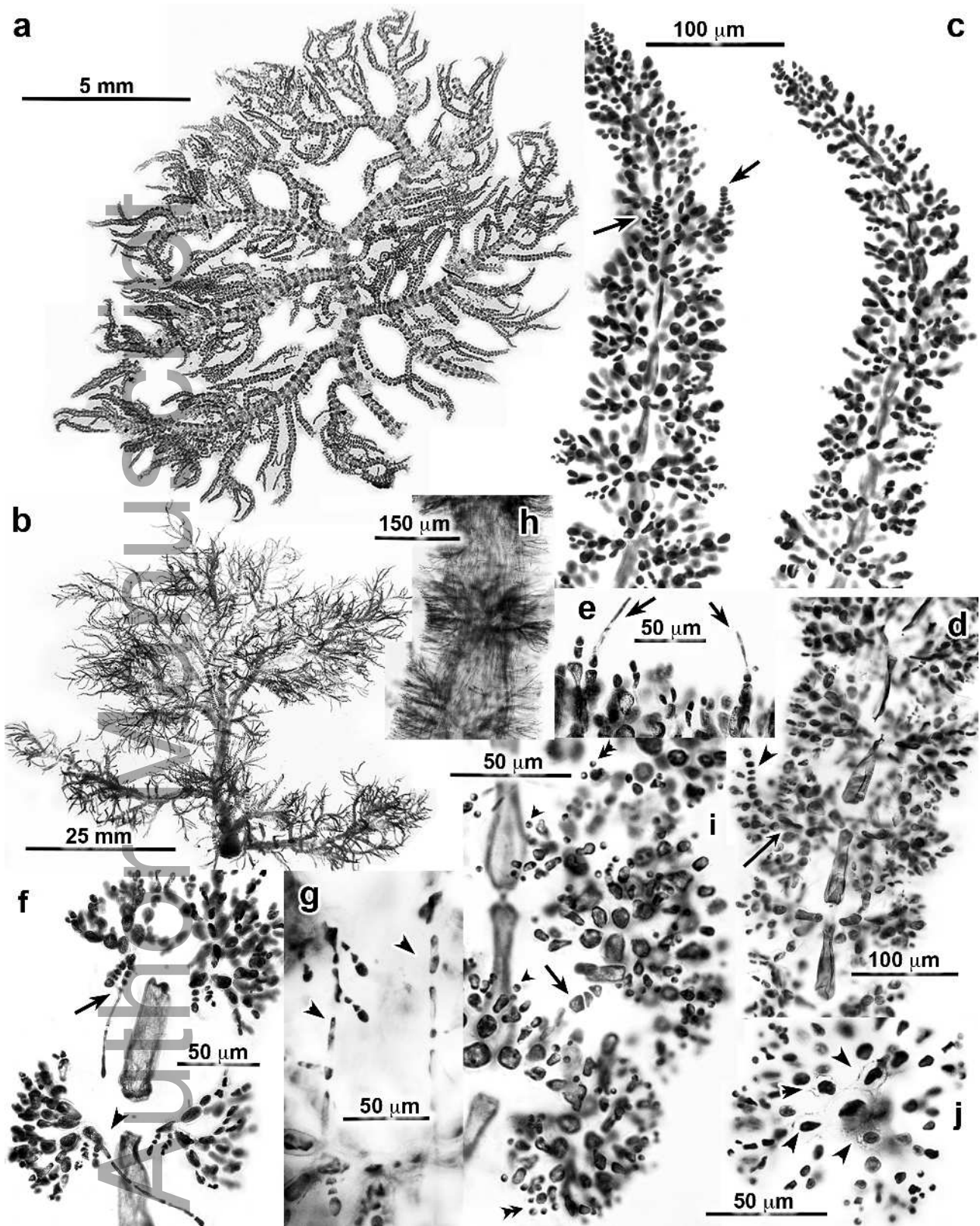


jpy_12426-16-002_f4.tif

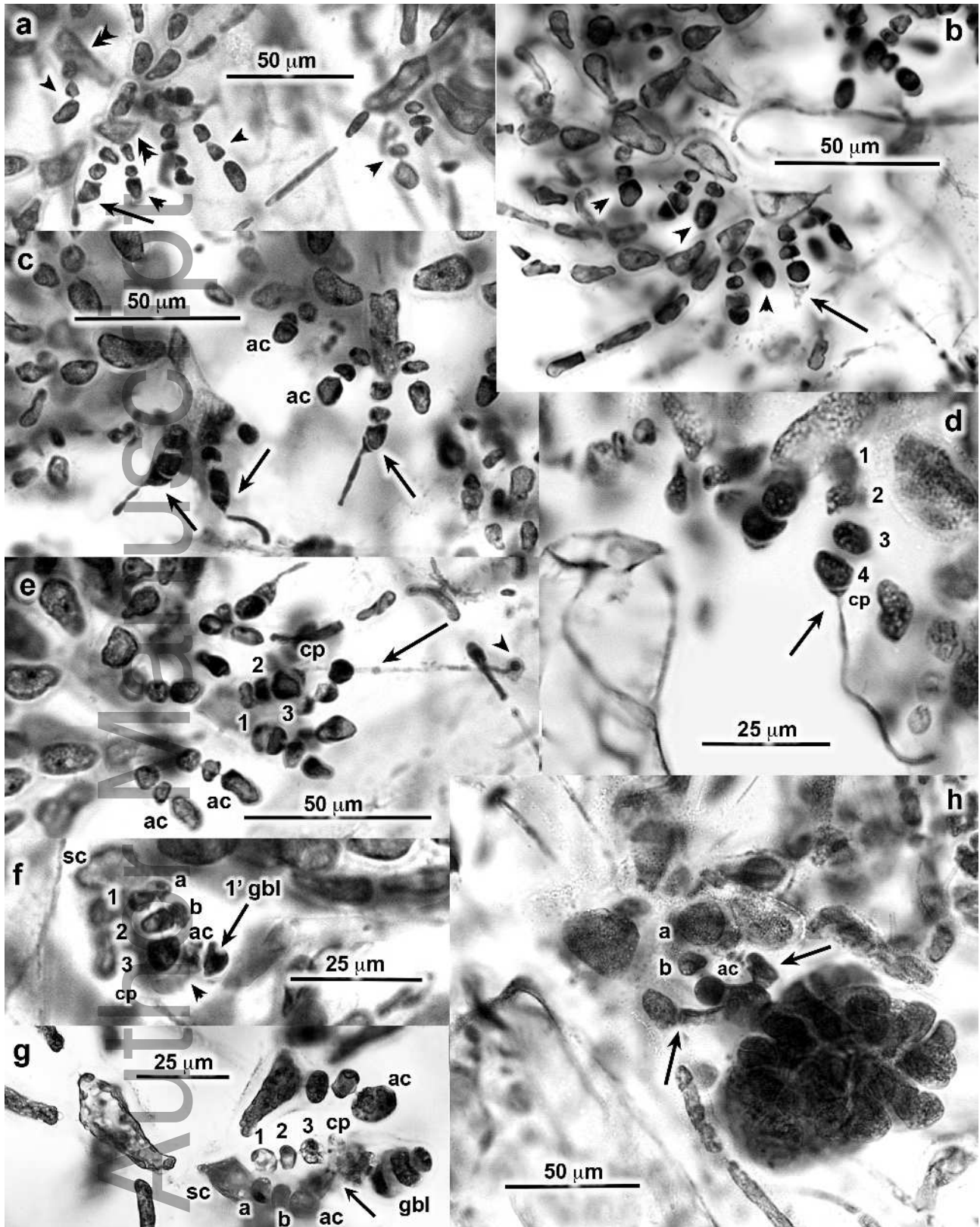
Author



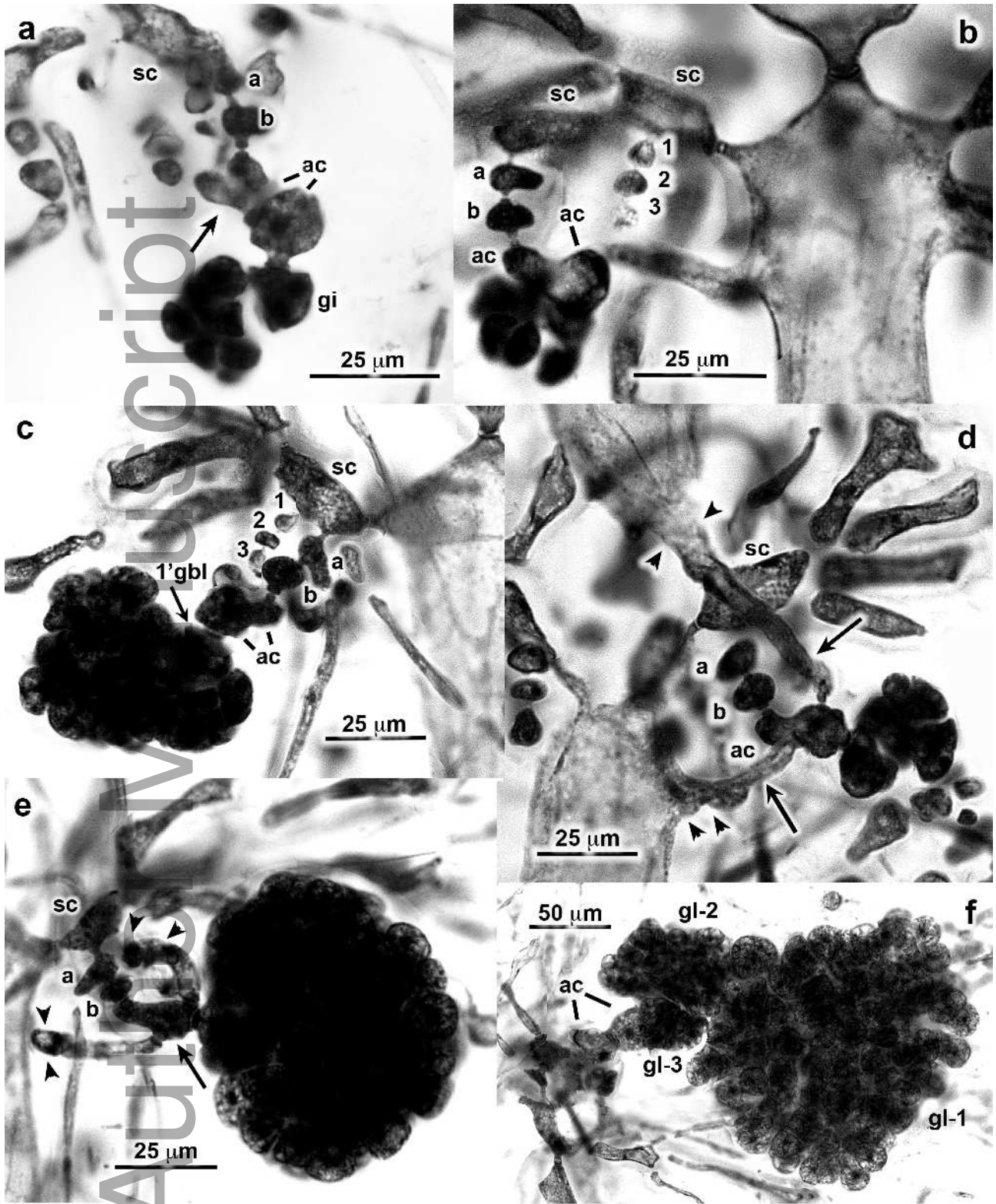
jpy_12426-16-002_f5.tif



jpy_12426-16-002_f6.tif



jpy_12426-16-002_f7.tif



jpy_12426-16-002_f8.tif